Wiley
International Journal of Biomaterials
Volume 2024, Article ID 5184399, 28 pages
https://doi.org/10.1155/2024/5184399

WILEY

Research Article

A Study on the Potential of Valorizing *Sargassum latifolium* into Biofuels and Sustainable Value-Added Products

Nour Sh. El-Gendy,[1,2] **Mohamed Hosny**,[1] **Abdallah R. Ismail**,[1] **Ahmad A. Radwan**,[3] **Basma A. Ali**,[4] **Hager R. Ali**,[1] **Radwa A. El-Salamony**,[1] **Khaled M. Abdelsalam**,[5] **and Manal Mubarak**[6]

[1]*Egyptian Petroleum Research Institute (EPRI), Nasr City, P.O. 11727, Egypt*
[2]*Center of Excellence, October University for Modern Sciences and Arts (MSA), 6th of October City, P.O. 12566, Egypt*
[3]*National Research Centre (NRC), El-Dokki, Cairo, P.O. 12622, Egypt*
[4]*General Organization for Export and Import Control (GOEIC), Cairo, Egypt*
[5]*Marine Environment Division, National Institute of Oceanography and Fisheries NIOF, Alexandria Branch, P.O. 21519, Egypt*
[6]*Soil and Water Department, Faculty of Agriculture, Ain Shams University, Cairo, P.O. 11241, Egypt*

Correspondence should be addressed to Nour Sh. El-Gendy; nshelgendy@msa.edu.eg

Received 20 January 2024; Revised 14 June 2024; Accepted 12 August 2024

Academic Editor: Kaliannan Durairaj

Copyright © 2024 Nour Sh. El-Gendy et al. This is an open access article distributed under the Creative Commons Attribution License, which permits unrestricted use, distribution, and reproduction in any medium, provided the original work is properly cited.

To increase the limited commercial utility and lessen the negative environmental effects of the massive growth of brown macroalgae, this work illustrates the feasibility of valorizing the invasively proliferated *Sargassum latifolium* into different value-added products. The proximate analysis recommends its applicability as a solid biofuel with a sufficient calorific value (14.82 ± 0.5 MJ/kg). It contains $6.00 \pm 0.07\%$ N + P_2O_5 + K_2O and $29.61 \pm 0.05\%$ organic C. Its nutritional analysis proved notable carbohydrate, ash, protein, and fiber contents with a rational amount of lipid and a considerable amount of beneficial macronutrients and micronutrients, with a low concentration of undesirable heavy metals. That recommends its application in the organic fertilizer, food, medicine, and animal fodder industries. A proposed eco-friendly sequential integrated process valorized its biomass into 77.6 ± 0.5 mg/g chlorophyll, 180 ± 0.5 mg/g carotenoids, 5.86 ± 0.5 mg/g fucoxanthin, 0.93 ± 0.5 mg/g β-carotene, $21.97 \pm 0.5\%$ (w/w) alginate, and $16.40 \pm 0.5\%$ (w/w) cellulose, with different industrial and bioprocess applications. Furthermore, *Aspergillus galapagensis* SBWF1, *Mucor hiemalis* SBWF2, and *Penicillium oxalicum* SBWF3 (GenBank accession numbers OR636487, OR636488, and OR636489) have been isolated from its fresh biomass. Those showed wide versatility for hydrolyzing and saccharifying its polysaccharides. A Gram-negative *Stutzerimonas stutzeri* SBB1(GenBank accession number OR764547) has also been isolated with good capabilities to ferment the produced pentoses, hexoses, and mannitol from the fungal saccharification, yielding 0.25 ± 0.014, 0.26 ± 0.018, and 0.37 ± 0.020 g ethanol/g algal biomass, respectively. Furthermore, in a pioneering step for valuing the suggested sequential biomass hydrolysis and bioethanol fermentation processes, the spent waste *S. latifolium* disposed of from the saccharification process has been valorized into C-dots with potent biocidal activity against pathogenic microorganisms.

1. Introduction

Climate change and its concomitant issues, such as rising seawater temperatures, have resulted in the progressive growth of brown macroalgae and their massive spread across the Red Sea shorelines [1]. *Sargassum* sp. is considered one of the main brown macroalgae that inhabit the Red Sea [2–4]. Overfishing activities, increased levels of nutrients and organic pollutants due to the open discharge of industrial effluents, and other activities related to the oil and gas industry contribute to the overgrowth of brown macroalgae [5]. The massive growth of brown algae leads to

eutrophication problems, reducing light penetration, and negatively affecting biodiversity and life underneath water [6]. Its multi-increment antagonistically competes with coral reefs, suffocating reefs, which accelerates reef degradation and causes coral bleaching and death [7]. Their massive growth also has the potential to entangle marine mammals and turtles [8]. Not only that, but their presence along shorelines also has a detrimental effect on turtle nesting [9]. In addition to creating issues with solid waste management, macroalgal blooming also produces hydrogen sulfide gas, which is poisonous and corrosive, creates piles on shorelines that may decay, forming a bad smell, and produces methane that rigorously adds to the problem of climate change [10] and leads to the invasion of insects that can irritate the skin [11]. Consequently, this causes harm to shorelines and has severe negative effects on aquaculture, the food chain, the marine ecosystem, tourism, and the economy [6].

Because of fast-growing globalization and industrialization, besides the worldwide exponential growth of the human population, the demand for different industrial feedstock, fertilizers, animal fodders, and energy has increased. Recently, among the sustainable resources, marine macroalgae have attracted researchers and the industrial sector as being a promising, readily available, and cost-effective feedstock for different industrial applications. They do not cause the food versus fuel problem; they do not require fertilizer, pesticides, fresh water, arable land, or farming lands for cultivation [12]. Because they grow quickly and produce a lot of biomass per area, and because they have low amounts of lignin and high amounts of carbohydrates, they show a lot of promise for use in biorefineries and the production of biofuels [13].

The utilization of *Sargassum* biomass as a feedstock in biorefineries for the production of various industrial value-added products, such as platform chemicals, animal feeders, and biofertilizers, besides third-generation biofuels, has recently attracted increased industrial interest [14].

In an attempt to overcome that issue and substantiate the perception that waste is not a waste until it is wasted, this work investigates the feasibility of *Sargassum latifolium* acting as a habitat for microorganisms capable of hydrolyzing, saccharifying, and fermenting its lignocellulosic biomass and carbohydrate constituents into fermentable sugars and bioethanol. It also studies the applicability of *Sargassum latifolium* as a precursor for organic fertilizer, animal fodder, primary solid biofuel, and C-dot with considerable biocidal activity against pathogenic microorganisms. Furthermore, it suggests an eco-friendly, fully integrated process for its valorization into pigments, antioxidants, alginate, and cellulose with various industrial applications.

2. Materials and Methods

2.1. Sampling of Macroalgal Biomass and Its Associated Water. The brown *Sargassum latifolium* biomass and its associated water sample have been collected from Hurghada city shoreline, Red Sea Governorate, Egypt, during the autumn season of 2022 (27°23′11″N 33°47′17″E) (Figure 1).

The microscopic examination of the collected *Sargassum latifolium* has been performed according to Liang et al. [15] and Yeh et al. [16] using a stereo microscope (Novex, model P-20, Euromex microscopes BV, Arnheim, the Netherlands) and a light microscope (Optika model B-192, S.r.l.Via Rigla, Ponteranica (BG), Italy).

Water analysis for the collected algal biomass-associated water was performed in the Egyptian Petroleum Research Institute's Central Analytical Labs, according to ASTM [17]. Anions and cations were determined according to ASTM D4327 [17] and ASTM D6919 [17] using ion chromatography (Thermo-Dionex™ ICS-6000 Capillary HPIC™ System equipped with high capacity columns AS9 and CS12 for anion and cations, respectively, Thermo Fisher Scientific, Carlsbad, California, USA). Heavy metals were determined according to ASTM D4691 [17] using a Flame Atomic Absorption Spectrophotometer (model ZEEnit 700 P, Analytik Jena GmbH, Hena, Germany). Total dissolved solids (TDS) and total suspended solids (TSS) were determined according to ASTM D5907 [17] for filterable matter (TDS) and nonfilterable matter (TSS) in water. Conductivity and resistivity were determined on-site according to ASTM D1125 [17] using a digital conductivity meter (model WTW 330i, Willis Towers Watson Public Limited Company, London, UK). Density and specific gravity were determined according to ASTM D1429 [17]. pH was determined according to ASTM D1293 [17] using a digital pH meter (model Mettler Toledo-Seven GoTM, Ohio, USA). Alkaline species (CO_3, OH, and HCO_3) were measured according to ASTM D3875 [17]. Alkalinity was determined according to ASTM D1067 [17]. The hardness value of water (Ca and Mg) was determined according to ASTM D6919 and calculated according to ASTM D1126 [17]. Biochemical oxygen demand (BOD) and chemical oxygen demand (COD) were measured according to APHA method 5210 [18] and ASTM D1252 [17], respectively. Salinity was calculated according to APHA method 2520 [18].

2.2. Macroalgal Biomass Preparation. After being gathered, the macroalgae were cleaned with tap water to remove any remaining dirt, salt, and sand. They were then left to dry in the sun. After that, they were homogenized into a 0.8–1 mm powder by grinding and sieving. Lastly, they were stored at room temperature until needed in clean, sealed plastic bags.

2.3. Physicochemical Characterization of the Collected Algal Biomass. The nutritional components of *S. latifolium* biomass were determined according to the techniques outlined in AOAC [19]. The proximate analysis, which involved measuring the calorific value [20], volatile matter [21], ash [22], and moisture [23] contents, has also been done. The method described by Moubasher et al. [24] has been used to determine the amounts of cellulose, hemicellulose, and lignin in the collected *S. latifolium* biomass. The biochemical analysis was conducted according to El-Gendy et al. [25]. The Walkley and Black method [26] was used to determine the concentrations of organic carbon and matter.

6418, 2024, 1, Downloaded from https://onlinelibrary.wiley.com/doi/10.1155/2024/5184399 by Egyptian National Sci. Network (Enstinet), Wiley Online Library on [25/10/2024]. See the Terms and Conditions (https://onlinelibrary.wiley.com/terms-and-conditions) on Wiley Online Library for rules of use; OA articles are governed by the applicable Creative Commons License

Figure 1: *Sargassum latifolium* on Egyptian Red Sea shoreline (27°23′11″N 33°47′17″E).

The Jackson [27] method was used for measuring the electrical conductivity and pH. The Kjeldahl digestion method, as reported by Chapman and Pratt [28], was utilized to quantify total N, and the crude protein concentration was computed using the conversion factor (6.25). The method of Watanabe and Olsen [29] was used to quantify total phosphorus. ICP-MS (inductively coupled plasma mass spectrometry, Spectro Ciros CCD ICP-OES, Spectro Analytical Instruments, Kleve, Germany) was used in accordance with the methodology outlined by Benton [30] to determine the minerals and heavy metal contents.

2.4. A Fully Integrated Process for Extraction of Various Value-Added Products from S. latifolium Biomass. The pigments and alginate were sequentially extracted from the algal biomass according to the method reported by Trica et al. [31], and then the cellulose was extracted from the leftover biomass according to the method reported by Trivedi et al. [32]. Figure 2 shows the whole integrated process that is sequentially used to extract various value-added products.

The extracted pigments were detected by scanning the distinctive absorption spectra at wavelengths of 190–800 nm using a UV/Vis/NIR double beam spectrophotometer (model V-570, JASCO International Co., Ltd., Tokyo, Japan) [33].

According to Ismail [33], the extracted concentration of chlorophyll a and β-carotene was calculated as follows;

$$\text{Total Chloropyll (mg/g)} = \frac{[20.2A_{645} + 8.02A_{663}] \times V}{W}, \quad (1)$$

$$\text{Carotenoids (mg/g)} = \frac{4A_{480} \times V}{W}. \quad (2)$$

The preliminary calculation of fucoxanthin concentration was done according to Ktari et al. [34]:

$$\text{Fucoxanthin (mg/g)} = \frac{[7.69 \times (A_{480} - A_{750}) - 5.55 \times [(A_{631} - A_{750}) + (A_{582} - A_{750}) - 0.297 \times (A_{665} - A_{750})] - 0.377 \times (A_{665} - A_{750})] \times V}{W}. \quad (3)$$

The preliminary calculation of β-carotene concentration was done according to Ismail et al. [35]:

$$\beta - \text{Carotene (mg/g)} = \frac{[0.216 \times A_{663} - 0.304 \times A_{450} + 0.452 \times A_{453}] \times \text{V}}{W}. \quad (4)$$

Fourier transform infrared (FTIR; Perkin Elmer Spectrum One, Waltham, MA, USA) was used according to the method reported by El-Gendy et al. [25] to characterize the extracted value-added products. The X-ray diffractometer (XRD) patterns and the average particle size of the extracted alginate and cellulose have been corroborated by high-resolution XRD (PANalytical X'PERT Pro MPD, Lelyweg, EA Almelo, the Netherlands) in conjunction with a Cu k radiation source ($\lambda = 1.5418$ Å) running at 40 kV and 40 mA and a dynamic light scattering device (DLS, Zetasizer Nano Series (HT), Nano ZS, Malvern Instruments, Malvern, UK), respectively. Their granule morphologies have been studied using a field emission scanning electron microscope embedded with smart energy dispersive X-ray spectroscopy (FESEM-EDX, model Sigma 300VP Carl Zeiss, Jena, Germany).

Furthermore, according to El-Gendy et al. [25], under nitrogen circumstances, Q600 SDT simultaneous differential scanning calorimetry-thermal gravimetric analysis (DSC–TGA) and the TA instrument Discovery DSC250 (New Castle, DE, USA) were used to investigate the thermal

6418, 2024, 1, Downloaded from https://onlinelibrary.wiley.com/doi/10.1155/2024/5184399 by Egyptian National Sci. Network (Enstinet), Wiley Online Library on [25/10/2024]. See the Terms and Conditions (https://onlinelibrary.wiley.com/terms-and-conditions) on Wiley Online Library for rules of use; OA articles are governed by the applicable Creative Commons License

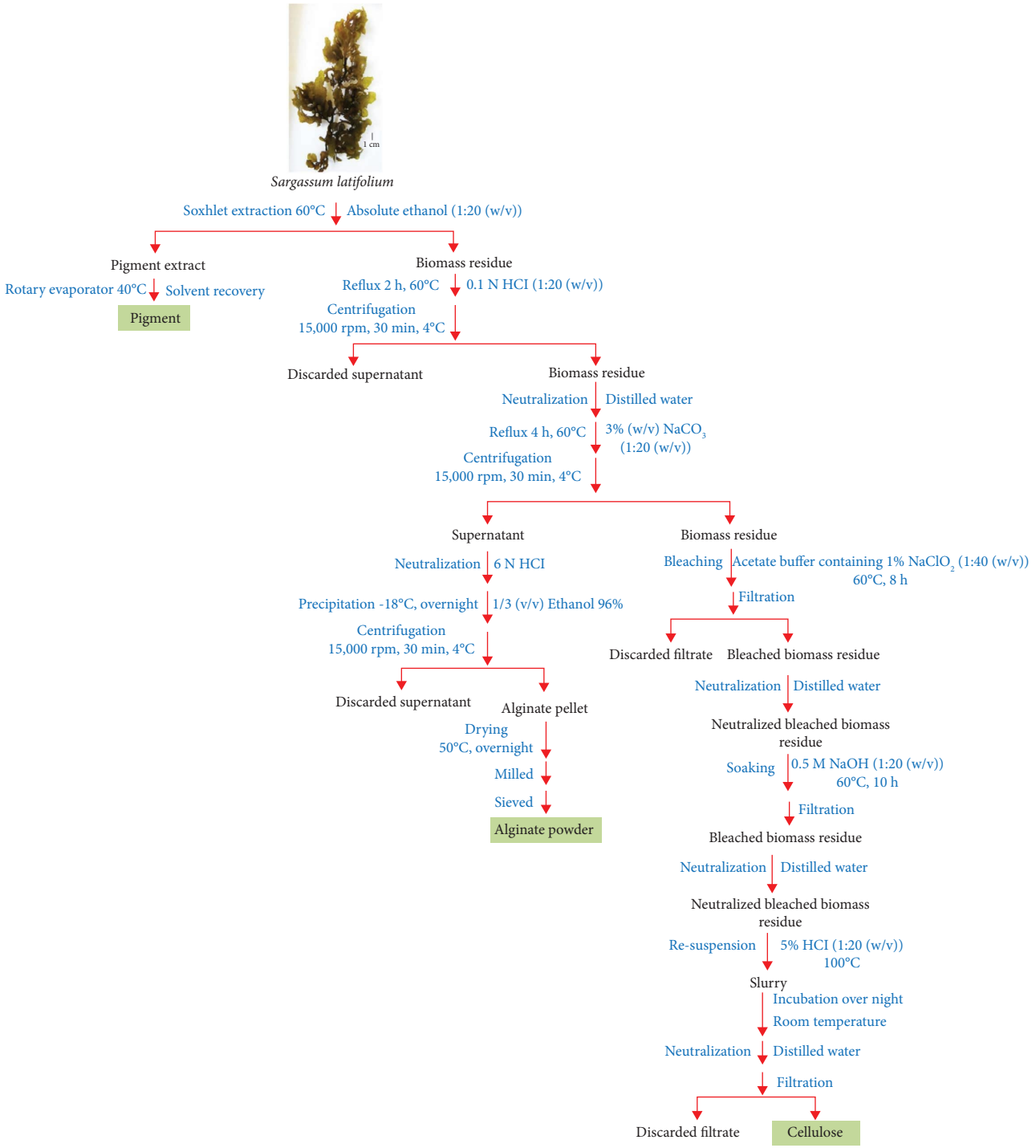

Figure 2: A fully integrated process for the production of value-added products from the collected *S. latifolium*.

properties of the value-added products and to generate their DSC data, respectively. The thermograms obtained were subjected to the analysis using TA Instruments Trios software (V5.2.2.47561, New Castle, DE, USA). Then, the integrated peak area was divided by the heating temperature rate (5°C/min) and the weight of the value-added product slurry (5 mg) in order to calculate the gelatinization enthalpy (ΔH J/g). For reproducibility, all analyses were done in triplicate.

2.5. Isolation of Microbial Strains Capable of Hydrolyzing and Saccharifying Different Algal Polysaccharides and Fermenting Different Di- and Monosaccharides. The microbial isolation has been performed from the freshly collected *S. latifolium* biomass and its associated water according to the method reported by Abo-State et al. [36]. Luria-Bertani (LB) medium with pH7 [37], Wickerham's (WH) medium with pH5.5 [38], and Sabouraud dextrose (SD) medium with pH5.5 [39] have been used for the isolation and maintenance of bacteria,

6418, 2024, 1, Downloaded from https://onlinelibrary.wiley.com/doi/10.1155/2024/5184399 by Egyptian National Sci. Network (Enstinet), Wiley Online Library on [25/10/2024]. See the Terms and Conditions (https://onlinelibrary.wiley.com/terms-and-conditions) on Wiley Online Library for rules of use; OA articles are governed by the applicable Creative Commons License

yeast, and fungi, respectively. In 250 mL conical flasks, 90 mL of sterile saline (8.5 g/L NaCl) was mixed with 10 g of fresh algal biomass under aseptic conditions. For sixty minutes, the flasks were shaken at 200 rpm. Subsequently, the suspensions were cultured on LB, WH, and SD agar plates for bacteria, yeast, and fungi, respectively, and serially diluted to 10^{-1}.

Inoculated LB and WH Plates were cultured for 48 hours, while the inoculated SD plates were cultured for seven days at 30°C. Then, the obtained well defined and separated colonies were streaked on a sterile, appropriate medium for purification. Fungal purification has been performed by adding 100 mg/L Rose Bengal to the Saboraud medium before sterilization.

The primary screening and evaluation of the performance of the obtained fungal isolates on different algal polysaccharides have been performed according to Bahkali [40]. The fungal isolate discs were incubated for 7 days at 30°C onto minimal-agar plates supplemented with 1% (w/v) of different polysaccharides, alginate, cellulose, and hemicellulose. Then, the growth was monitored and tabulated.

The screening and evaluation of the performance of the obtained fungal isolates to hydrolyze and saccharify the collected *S. latifolium* biomass have been performed according to Abo-State et al. [36]. The fungal isolates were inoculated in a final concentration (5% w : w) onto sterilized wet algal biomass (25% w/v biomass : distilled H_2O), and then statically incubated for 7 days at 30°C. The produced sugars were then extracted by 50 mL distilled H_2O and quantified by the 3,5-dinitrosalicylic acid (DNS) method [41]. The total reducing sugar (TRS) yield (mg TRS/g algal biomass) and saccharification efficiency were then calculated according to Soliman et al. [12]:

$$\text{Yield (mg/g)} = \frac{\text{TRS mg}}{\text{Algal biomass dry weight g}}, \tag{5}$$

$$\text{Sacrification \%} = \left(\frac{\text{Released TRS g} \times 0.9}{(\text{Algal cellulose} + \text{Algal hemicellulose})\ \text{g}}\right) \times 100. \tag{6}$$

The conversion percentage was calculated according to Kooren et al. [18]:

$$\text{Conversion \%} = \left(\frac{\text{TRS g}}{\text{Algal biomass dry weight g}}\right) \times 100. \tag{7}$$

The screening of the capability of different microbial isolates to ferment wide varieties of di- and monosaccharides has been performed according to Abo-State et al. [36]. All the yeast and bacterial isolates were streaked separately onto minimal-agar plates [40] supplemented with 1% (w/v) of different saccharides, and then incubated for 48 h at 30°C. Finally, the growth was monitored and tabulated. The sugars used for this test were mannitol as representative for sugar alcohol; xylose and arabinose as representative for reducing pentoses; glucose, mannose, galactose, and fructose as representative for reducing hexoses; lactose and maltose as representative for reducing disaccharides; and sucrose as representative for nonreducing disaccharides.

2.6. Identification of the Obtained Microbial Isolates. The bacterial isolates were molecularly identified by 16S ribosomal RNA gene sequence using two sets of universal primers, 27F (AGAGTTTGATCMTGGCTCAG) and 1492R (TACGGYTACCTTGTTACGACTT), amplifying about 1465 bp of the 16S rDNA region [42]. For the molecular identification of the isolated yeast and fungi, the internal transcribed spacer regions in 18S ribosomal RNA, ITS1 (CTTGGTCATTTAGAGGAAGTAA) and ITS4 (TCCTCC GCTTATTGATATGC), were used to amplify 400–600 bp containing the complete sequence of the 5.8S rRNA gene and ITS 2 [43, 44]. Genomic DNA of bacteria and yeast was extracted using the GeneJET Genomic DNA Purification Kit (Thermo Fisher Scientific, USA) according to the manufacturer's instructions, whereas DNA of fungi was extracted by the CTAB method [45]. PCR was performed by adding 40 ng of extracted DNA in 50 mL of the PCR reaction solution (1 U of DreamTaq DNA polymerase (Thermo Fisher Scientific, USA), 1x buffer, 0.2 mM dNTPs, and 10 pmol of the appropriate primers). PCR products were purified by the GeneJET Gel Extraction Kit (Thermo Fisher Scientific, USA), and the purified DNA has been sent to GATC Biotech Company (Ebersberg, Germany) for sequencing. The selected efficient isolates were then identified based on their obtained 16S rDNA and ITS region sequence (query sequence) analysis on the NCBI server https://www.ncbi.nlm.nih.org, for bacteria, yeast, and fungi, respectively, via the BLAST tool of the NCBI https://blast.ncbi.nlm.nih.gov/blast.cgi. The phylogenetic tree was then constructed using the maximum likelihood (ML) algorithms by MEGA 11.0.13 software after muscle alignment with 500 bootstrapping trials.

2.7. Identification and Quantification of the Produced Fermentable Sugars. Identification of sugar profile and their quantification in the produced hydolyzates have been performed as previously described by Abo-State et al. [36], using the high performance liquid chromatography (HPLC) model Agilent 1200 series USA equipped with a refractive

6418, 2024, 1, Downloaded from https://onlinelibrary.wiley.com/doi/10.1155/2024/5184399 by Egyptian National Sci. Network (Enstinet), Wiley Online Library on [25/10/2024]. See the Terms and Conditions (https://onlinelibrary.wiley.com/terms-and-conditions) on Wiley Online Library for rules of use; OA articles are governed by the applicable Creative Commons License

index RI detector model (Agilent 1260 infinity, Santa Clara, CA, USA) and a SUPELCOSIL-LC-NH_2 (25 cm × 4.6) column.

2.8. Screening the Capability of the Obtained Microbial Isolates for Bioethanol Production. The screening was performed according to the method reported by Abo-State et al. [36] on a mixture of representative model sugars (glucose, xylose, and mannitol) for hexoses, xyloses, and alcoholic sugars, respectively, besides the produced algal hydrolyzate. After adding peptone (10.0 g/L), KH_2PO_4 (2.0 g/L), and $MgSO_4$.7 H2O (1.0 g/L) to the model sugary solution or hydrolyzate, the mixture was autoclaved for 20 minutes at 121°C to sterilize it. 10% (v/v) of the microbial isolates were added to the medium as an inoculant. The inoculated cultures were then incubated for 48 hours at 150 rpm at 30°C. Finally, the fermented medium was centrifuged for 10 minutes at 10,000 rpm. The residual TRS were quantified by the DNS method [41] and the sugars' profile before and after fermentation was determined by the HPLC analysis according to the method reported by Abo-State et al. [36]. The produced ethanol was quantified according to the method described by Soliman et al. [12] using gas chromatography (model 6890; Agilent), equipped with a flame ionization detector and a nominal capillary column (60 m × 530 μm × 5.00 μm). Noninoculated flasks were used as −ve control and subjected to all experimental conditions as inoculated ones.

Bioethanol yield was calculated according to Zeng et al. [46]:

$$\text{Bioethanol yield} = \frac{\text{Concentration of produced bioethanol (g/L)}}{\text{Algal biomass (g/L)}}. \tag{8}$$

Actual bioethanol yield was calculated according to Jeyakumar et al. [47]:

$$\text{Actual biothanol yield} = \frac{\text{Concentration of produced bioethanol (mg/L)}}{\text{Initial Concentration of sugars (mg/L)}}. \tag{9}$$

Bioethanol conversion yield was calculated according to Aparicio et al. [48]:

$$\text{Biothanol conversion yield \%} = \left(\frac{\text{Concentration of produced bioethanol (mg/L)}}{\text{Initial Concentration of sugars (mg/L)}}\right) \times 100. \tag{10}$$

2.9. The Macroalgal Synthesis of Carbon-Dot. To maximize the value of the process, the spent waste *S. latifolium* disposed of from the bioethanol production process was used in a groundbreaking step to hydrothermally prepare the carbon-dot (CD) according to the method reported by Kumar et al. [49]. In a 150 mL Teflon-lined stainless steel autoclave, 10 g of the spent waste *S. latifolium* were combined with 100 mL of distilled water. The reaction mixture was heated at 180°C for 4 hours at a steady temperature until a dark brownish solution was produced. The reaction mixture was cooled to ambient temperature. To remove large unreacted particles, the obtained yellowish-brown solution was filtered through a Whatman 42 filter paper. To solubilize the produced CD and improve fluorescence, the solution was centrifuged at 5000 rpm for 20 minutes before being suspended in 5 ml of 1 N NaOH. Then, the aforementioned solution was dialyzed against pure water for 24 hours to purify the obtained CD.

The photoluminescence characteristics of the produced CD were determined at room temperature using a spectrofluorometer (JASCO FP-6500, Jasco International Co., Ltd., Tokyo, Japan) with an excitation wavelength set at $\lambda = 254$ nm. The produced CD was also characterized by the SENTERRA II Dispersive Raman Microscope (Bruker Optics, Billerica, MA, USA), Fourier transform infrared (FTIR; Perkin Elmer Spectrum One, Shelton, CT, USA), field emission scanning electron microscope-embedded smart energy dispersive X-ray spectroscopy (FESEM-EDX, model Sigma 300VP Carl Zeiss, Jena, Germany), and high-resolution transmission electron microscope (HRTEM, JEOL-JEM 2100F, 80–200 kV, Tokyo, Japan). The biocidal activity of the produced CD against pathogenic microorganisms was evaluated according to El-Gendy et al. [25].

The activity index was calculated according to El-Gendy et al. [25]:

6418, 2024, 1, Downloaded from https://onlinelibrary.wiley.com/doi/10.1155/2024/5184399 by Egyptian National Sci. Network (Enstinet), Wiley Online Library on [25/10/2024]. See the Terms and Conditions (https://onlinelibrary.wiley.com/terms-and-conditions) on Wiley Online Library for rules of use; OA articles are governed by the applicable Creative Commons License

$$\text{Activity index} = \frac{\text{CD inhibition zone (mm)}}{\text{Standard antibiotic inhibition zone (mm)}}. \quad (11)$$

2.10. Statistical Analysis. A Tukey-test, using SPSS software version 13.0 (Informer Technologies, Inc., Los Angeles, CA, USA) was performed to determine the significant difference between the acquired data, with a p value of greater than 0.05 considered nonsignificant at the 95% confidence level.

3. Results and Discussion

3.1. Morphological Analysis of the Collected Brown Macroalgae. The visual observation of the collected brown macroalgae (Figure 3) matches well with the previously published marine brown macroalgal species *Sargassum latifolium* collected from the Red Sea at the Kingdom of Saudi Arabia (KSA) Umluj shore [50], KSA Jeddah coast [2], Egypt Hurghada shoreline [51, 52], Egypt Ras Ghareb coast [12], and Egypt Ras Sedr coast [3]. *Sargassum latifolium* belongs to the *Phylum Ochrophyta, Class Phaeophyceae, Order Fucales*, and *Family Sargassaceae*. The collected thallus was found to reach up to 70 cm in height. It has spherical, obovate, and pyriform air-vesicles that are stalked with serrated wings and without any projections (Figure 3). It has spiny axes (blue arrows, Figure 3). It has lanceolate leaves with seriated edges, a leathery texture, and randomly distributed cryptostomata (Figure 3). The stereomicroscopy examination of the axis (Figure 4) shows the paraphyses or mucilage hairs, which are known to be responsible for mucilage secretion and also the absorption of minerals and water. The microscopic examination of the transverse sections of *Sargassum latifolium* blades or leaves (Figure 5(a)) with their female conceptacle (Figure 5(b)) and male conceptacle (Figure 5(c)) is also illustrated and reveals the presence of oogonia and antheridia, which are responsible for sexual reproduction.

3.2. The Physicochemical Analysis of the Associated Water for the Collected Brown S. latifolium. The data illustrated in Table 1 summarize the physicochemical analysis of the algal biomass collected water and are comparable to those reported for Egyptian Red Sea water associated with *S. latifolium* [3] and *S. aquifolium* [1]. The observed high metal content might be related to the released metals from sediments, anthropogenic sources due to coastal region human activities, disposed industrial effluents, and other activities related to the oil and gas industry in that area [12]. The recorded pH and salinity matched those reported for the Red Sea by Abu Ahmed et al. [3]. The recorded oil content of approximately 11.85 mg/L might indicate oil pollution.

According to biological response values that may accompany or follow oil pollution, lethal effects range from 1 to 10 mg/L, but sublethal effects can be as low as 1 mg/L [53]. The recorded BOD of 48.4 mg/L (Table 1) might indicate organic pollution. Healthy water streams are characterized by a BOD <2 mg/L, while polluted ones have a BOD ≥10 mg/L [54]. The relatively high concentrations of nitrite and nitrate (Table 1) would enhance the growth and proliferation of macroalgae [55]. The low concentrations of ammonium and phosphate (Table 1) would confirm the overgrowth of macroalgae, as they are considered the major nutrients consumed during their primary growth and proliferation [54].

3.3. The Physicochemical Analysis of the Collected Brown S. latifolium. The tabulated proximate analysis of S. *latifolium* biomass (Table 2) depicts a sufficient calorific value of 14.82 ± 0.5 MJ/kg. That is as good as those reported for *Sargassum* [56] and lignocellulosic [57] biomass. Furthermore, the undesirable ash (Table 2) and heavy metal (Table 3) contents were low and within the permissible levels recommended by the International Organization for Standardization [58]. Thus, it can be utilized as a primary solid biofuel.

The recorded cellulose, hemicellulose, and lignin contents (Table 2) for the collected *S. latifolium* biomass in this study are comparable to the previously reported data for *Sargassum* spp. [50, 60], which recorded $20.35 \pm 0.5\%$ and $15.41 \pm 0.5\%$ for cellulose, $25.73 \pm 0.5\%$ and $25.43 \pm 0.5\%$ for hemicellulose, and $6.95 \pm 0.5\%$ for lignin. The holocellulose content of approximately $40.5 \pm 0.5\%$ aligns with the reported range of 40% to 60% for *Sargassum* species [61].

The nutritional analysis illustrated in Table 2 shows that the collected brown *S. latifolium* biomass has notable carbohydrate, ash, protein, and fiber contents with a rational amount of lipid, recording $41.5 \pm 0.5\%$, $24 \pm 0.5\%$, $15.94 \pm 0.31\%$, $7.98 \pm 0.5\%$, and $1.38 \pm 0.05\%$ (w/w), respectively. These values were comparable to those reported for *Sargassum* sp. [65]. Moreover, it has a considerable amount of beneficial macronutrients and micronutrients, recording 508.46 ± 0.2 mg/kg and 44.95 ± 0.2 mg/kg, respectively, with a low concentration of undesirable heavy metals, recording 989.9 ± 0.25 μg/kg (Table 3). That suggests using it not only medicinally as a multivitamin source and in food supplements [62], but also in animal fodder production [63, 64] and food manufacturing [65].

The recorded concentrations of undesirable heavy metals, Pd, Cd, and Hg (Table 3), were comparable to those reported by Lee et al. [10] for different collected *Sargassum* species. The carbohydrate and ash contents of the collected *S. latifolium* in this study (Table 2) were comparable to those reported by Fouda et al. [52] and Abu Ahmed et al. [3]. However, the recorded protein and fiber contents (Table 2) were higher. But they were comparable to those reported for *S. binderi*, which is recommendable for poultry diets [66]. Moreover, the carbohydrate and lipid contents (Table 2) were comparable to those of Egyptian *S. latifolium* [67], which recorded 41.08% and 1.13%, respectively.

The data in Tables 3 and 4 closely match the Egyptian organic fertilizer standard, with $N + P_2O_5 + K_2O$ and organic C contents of $6.00 \pm 0.07\%$ and $29.61 \pm 0.05\%$, respectively,

6418, 2024, 1, Downloaded from https://onlinelibrary.wiley.com/doi/10.1155/2024/5184399 by Egyptian National Sci. Network (Enstinet), Wiley Online Library on [25/10/2024]. See the Terms and Conditions (https://onlinelibrary.wiley.com/terms-and-conditions) on Wiley Online Library for rules of use; OA articles are governed by the applicable Creative Commons License

Figure 3: Normal visual examination of the collected brown *Sargassum latifolium*.

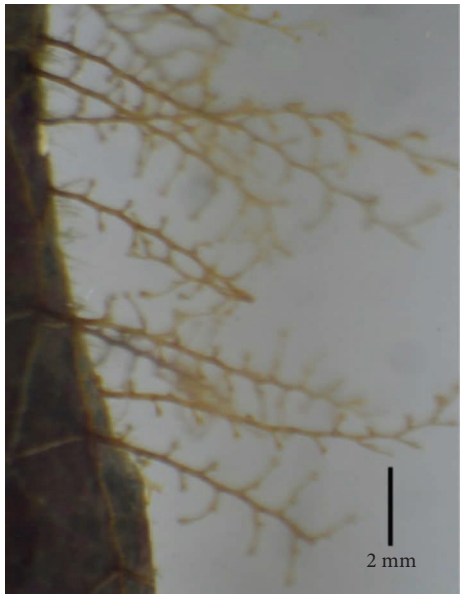

Figure 4: Stereo zoom microscopic examinations showing the paraphyses on the axis of the collected brown *Sargassum latifolium*.

suggesting its suitability for organic fertilizer production. Different *Sargassum* species *S. vulgare* [68, 69], *S. polycystum* [70], *S. horneri* [71], and *Sargassum* sp. [72] have been reported for the production of organic fertilizer.

The recorded relatively high carbohydrates, cellulose, and hemicellulose contents, with a relatively low lignin content of approximately $41.5 \pm 0.5\%$, $15.5 \pm 0.5\%$, $25 \pm 0.5\%$, and $8.2 \pm 0.5\%$, respectively (Tables 2), recommend the applicability of the collected *S. latifolium* biomass in the production of liquid biofuels and different biorefineries [12, 25, 73], besides the food, cosmetics, and pharmaceutical industries [56].

3.4. A Fully Integrated Process for Extraction of Various Value-Added Products from S. latifolium Biomass

3.4.1. The Pigments and Antioxidants. The ethanol extraction yielded pigments and antioxidants mixture of approximately $6.74 \pm 0.5\%$ (w/w). The UV/Vis spectrum of the obtained extract (Figure 6) matched that reported by Indrawati et al. [74] for *Sargassum* sp. pigment extract. It proved the presence of fucoxanthin antioxidant in the ethanol extract of *S. latifolium* macroalgae, besides some other important pigments and antioxidants: chlorophyll-a and -b, β-carotene, phycoerythrin, and phycocyanin. These findings are comparable to those reported for *S. binderi* [75]. The characteristic peaks of chlorophyll-a and -b appear at λ_{662nm} and λ_{645nm} [76, 77], with the predominance of chlorophyll-a. That coincides with the extract of brown macroalgae, *Saccharina latissima* [77]. The carotenoids with their predominant peak and β-carotene

6418, 2024, 1, Downloaded from https://onlinelibrary.wiley.com/doi/10.1155/2024/5184399 by Egyptian National Sci. Network (Enstinet), Wiley Online Library on [25/10/2024]. See the Terms and Conditions (https://onlinelibrary.wiley.com/terms-and-conditions) on Wiley Online Library for rules of use; OA articles are governed by the applicable Creative Commons License

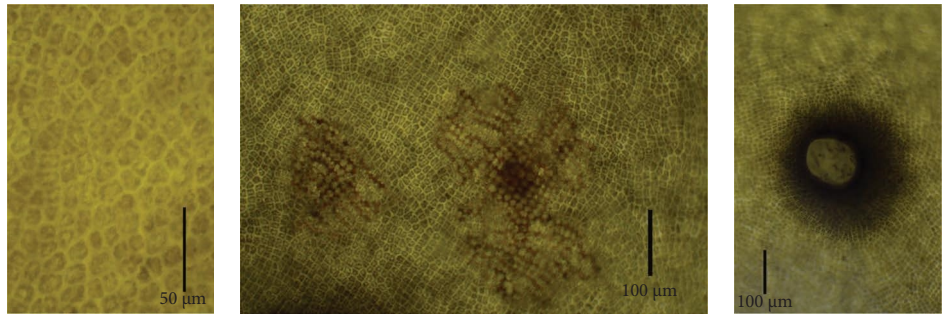

(a) (b) (c)

FIGURE 5: Microscopical examination for different transverse sections of the collected brown *Sargassum latifolium*: (a) medullar cells, (b) female conceptacles, and (c) male conceptacle.

TABLE 1: Water analysis for the collected *S. latifolium* biomass-associated water.

Physical and chemical properties			
Total dissolved solids (TDS)	35298.0 mg/L	Density @ 60 F	1.02847 g/mL
Salinity (as NaCl)	39475.9 mg/L	Specific gravity	1.02949
Alkalinity (as $CaCO_3$)	128.3 mg/L	pH @ 25°C	7.69
Total hardness (as $CaCO_3$)	6280.2 mg/L	Conductivity	5.55×10^{-2} mohs/cm @ 25°C
BOD	48.4 mg/L	Resistivity	0.1802 ohm-m @ 25°C
COD	56.3 mg/L	Oil content	11.85 mg/L

Inorganic chemical constituents					
Cation	mg/L	meq/L	Anion	mg/L	meq/L
Lithium	0.13	0.019	Fluoride	165.60	8.717
Sodium	10918.77	474.748	Chloride	19076.32	537.380
Ammonium	22.55	1.250	Bromide	487.56	6.104
Potassium	352.67	9.021	Nitrate	233.04	3.759
Magnesium	1257.64	103.491	Nitrite	280.01	6.074
Calcium	441.02	22.007	Phosphate	Nil	Nil
Strontium	Nil	Nil	Sulfate	1859.93	38.742
Barium	46.27	0.674	Hydroxide	Nil	Nil
Iron	Nil	Nil	Carbonate	Nil	Nil
Copper	Nil	Nil	Bicarbonate	156.47	2.564

TABLE 2: Algal biomass analysis.

Proximate analysis				
Moisture content %	Volatile content %	Fixed carbon %	Ash content %	Calorific value MJ/kg
9.2 ± 0.3	66 ± 0.5	0.8 ± 0.05	24 ± 0.5	14.82 ± 0.5

Biochemical analysis %			
Hemicellulose	Cellulose	Lignin	Ash
25 ± 0.5	15.5 ± 0.5	8.2 ± 0.5	24 ± 0.5

Nutritional composition Wt.% (w:w)					
Moisture content	Protein content	Fiber content	Carbohydrate content	Lipid content	Ash content
9.2 ± 0.3	15.94 ± 0.31	7.98 ± 0.5	41.5 ± 0.5	1.38 ± 0.05	24 ± 0.5

appear in the blue range between λ_{400nm} and λ_{500nm} [76]. The characteristic peaks of different valuable antioxidants also appear: fucoxanthin at λ_{330nm} and λ_{420nm} [76, 77], phycoerythrin at λ_{270nm}, λ_{308nm}, λ_{497nm} [78], and λ_{540nm}, while phycocyanin at λ_{618nm} [78], with predominance of fucoxanthin. Sanger et al. [79] reported the presence of chlorophyll (a, b, and C1 + C2), fucoxanthin, carotenoids, phycocyanin, and phycoerythrin in *Sargassum* species.

The chlorophyll and carotenoids recorded 77.6 ± 0.5 mg/g and 180 ± 0.5 mg/g, respectively. The fucoxanthin and β-carotene concentrations were found to be 5.86 ± 0.5 mg/g and 0.93 ± 0.5 mg/g, respectively.

The predominance of chlorophyll-a and fucoxanthin in the extract of *S. latifolium* has been previously reported by Ismail et al. [35]. The predominance of fucoxanthin over phycoerythrin and phycocyanin has also been reported for

6418, 2024, 1, Downloaded from https://onlinelibrary.wiley.com/doi/10.1155/2024/5184399 by Egyptian National Sci. Network (Enstinet), Wiley Online Library on [25/10/2024]. See the Terms and Conditions (https://onlinelibrary.wiley.com/terms-and-conditions) on Wiley Online Library for rules of use; OA articles are governed by the applicable Creative Commons License

Table 3: Mineral composition of the algal biomass.

	Macronutrients					Micronutrients					Undesired heavy metals				
	P	K	Ca	Mg	Fe	Zn	Mn	Cu	Ni	Cd	Cr	Pb	As	Hg	Co
	mg/kg					mg/kg						mg/kg			
S. latifolium	41.7 ± 0.05	208 ± 0.05	214.4 ± 0.05	44.36 ± 0.05	12.63 ± 0.05	24.53 ± 0.05	7.55 ± 0.05	0.24 ± 0.05	0.3021 ± 0.05	0.31 ± 0.05	0.0292 ± 0.05	0.0232 ± 0.05	0.0002 ± 0.0001	0.0002 ± 0.0001	0.325 ± 0.05
Egyptian organic fertilizer standard 8079/2017	—	—	—	—	—	Max 300	—	Max 100	Max 180	Max 5	Max 300	Max 300	—	Max 4	Max 100
Solid biofuels ISO 17225-1	—	—	—	—	—	≤100		≤20	≤10	≤0.5	≤50	≤10	≤1	—	—

6418, 2024, 1, Downloaded from https://onlinelibrary.wiley.com/doi/10.1155/2024/5184399 by Egyptian National Sti. Network (Enstinet), Wiley Online Library on [25/10/2024]. See the Terms and Conditions (https://onlinelibrary.wiley.com/terms-and-conditions) on Wiley Online Library for rules of use; OA articles are governed by the applicable Creative Commons License

Table 4: Physicochemical scrutiny of the algal biomass relative to the Egyptian organic fertilizer standard.

Parameter	*Sargassum latifolium*	Egyptian organic fertilizer standard (8079/2017)
Electrical conductivity dS/m	3.37 ± 0.05	6–10
Total dissolved solids (mg/L)	2157 ± 31.8	3840–6400
Organic C %	29.61 ± 0.05	Min 15
Organic matter %	50.92 ± 0.1	Min 18
Moisture content %	9.2 ± 0.3	Max 70
Total nitrogen %	2.55 ± 0.05	Min 0.28
P_2O_5 %	0.955 ± 0.01	Min 0.8
K_2O %	2.496 ± 0.01	Min 0.8
$N + P_2O_5 + K_2O$ %	6.00 ± 0.07	Min 4
C/N	11.61 ± 0.2	18–22 : 1
pH	7.5 ± 0.2	6–8

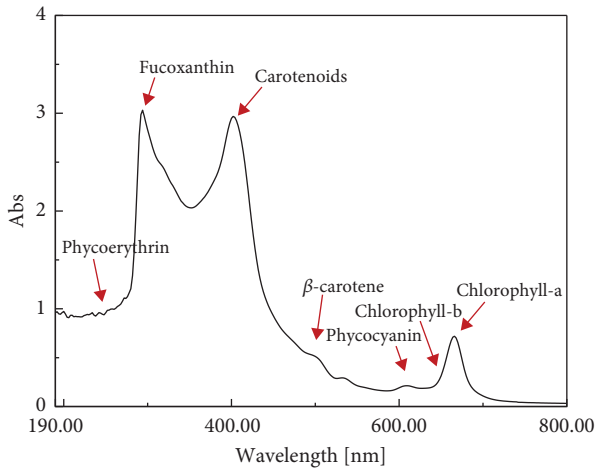

Figure 6: UV/Vis spectrum of *S. latifolium* ethanol extract.

the ethanol extract of *Sargassum* sp. [79]. Fucoxanthin is considered one of the major carotenoids in *Sargassum* species [80, 81]. It is known to be stable in normal storage conditions, and it has health-enhancing properties. It has many applications in the pharmaceutical and cosmetic industries, and it can also be applied as a bioingredient and functional food [81, 82].

3.4.2. Alginate Yield and Characterization. The collected *S. latifolium* yielded a pale yellow-colored alginate of approximately 21.97 ± 0.5% (w/w). This is higher than that previously published for *S. latifolium* [67, 83], which recorded 17.5%. However, *S. filipendula* [84], *Sargassum* sp. [85], and *S. muticum* [86] reported similar values of 24%, 24.56%, and 24.66%, respectively. According to Kok and Wong [87], the yield of alginate differs according to the season of algal harvesting, algal species, and method of extraction. *S. angustifolium* alginate ranged between 22.8% and 24.4% within the winter and summer, respectively [88]. According to Dharmayanti et al. [89], the alginate yield depends on the habitat itself, the sea tides, light intensity, and the available aquatic nutrients.

The XRD pattern of the alginate extracted from the collected *S. latifolium* (Figure 7(a)) is similar to that published by Benfares et al. [90]. It would indicate, according to Dalal et al. [67], the semicrystalline nature of the extracted alginate. According to Aprilliza [91], brown algae alginate has a semicrystalline structure. Such crystallinity in the extracted alginate might be, according to Kavitha et al. [92], attributed to the robust intermolecular interactions within the alginate chains via hydrogen bonding, which, according to Fang et al. [93], would differ depending on the algal species. The diffraction peaks appear around 2Θ of 26°, 30°, 32.5°, and 37° (Figure 7(a), green arrows) and are related to the 110 and 200 reflection planes of polyguluronate and polymannuronate units, respectively [94]. Other peaks that appeared around 45.5° and 52.5° also appeared in the XRD patterns of different seaweed alginates [94] and are related, according to Sundarrajan et al. [95], to the presence of other amorphous halos.

The FTIR analysis (Figure 7(b)) showed the characteristic peaks of alginate, which appear between 1080 cm^{-1} and 840 cm^{-1}. The FTIR spectrum (Figure 7(b)) is also matched with alginate extracted from *S. duplicatum*, *S. crassifolium*, and *S. pilulifera* [96, 97]. The symmetric stretching vibration of carboxylate groups is obvious at 1400 cm^{-1} with the presence of the asymmetric stretching vibration O-C-O at 1600 cm^{-1}. The vibration peaks around 1080 cm^{-1} and 1030 cm^{-1} would indicate the presence of guluronic and mannuronic units, respectively [6]. That is also confirmed by the presence of the peak of uronic acid C-O stretching vibration around 950 cm^{-1} and another small shoulder peak around 780 cm^{-1}. In addition, the vibrational peak of β-mannuronic acid residues appears around 820–880 cm^{-1} [98]. The peak that appears around 900 cm^{-1} is related to the C–H deformation vibration of α-L guluronic acid. Moreover, the broad hydrogen-bonded O–H stretching vibration and C–H stretching vibration appear at 3000–3200 cm^{-1} and 2920 cm^{-1}, respectively [6]. While the peak around 2460 cm^{-1} might be related to C-H of proteins [99]. The absence of peaks around 1200 cm^{-1} and 600 cm^{-1}, which are related to the symmetric and asymmetric O=S=O in sulfated polysaccharides [100], might indicate the purity of the extracted alginate and the absence of laminarin or fucoidan

6418, 2024, 1, Downloaded from https://onlinelibrary.wiley.com/doi/10.1155/2024/5184399 by Egyptian National Sci. Network (Enstinet), Wiley Online Library on [25/10/2024]. See the Terms and Conditions (https://onlinelibrary.wiley.com/terms-and-conditions) on Wiley Online Library for rules of use; OA articles are governed by the applicable Creative Commons License

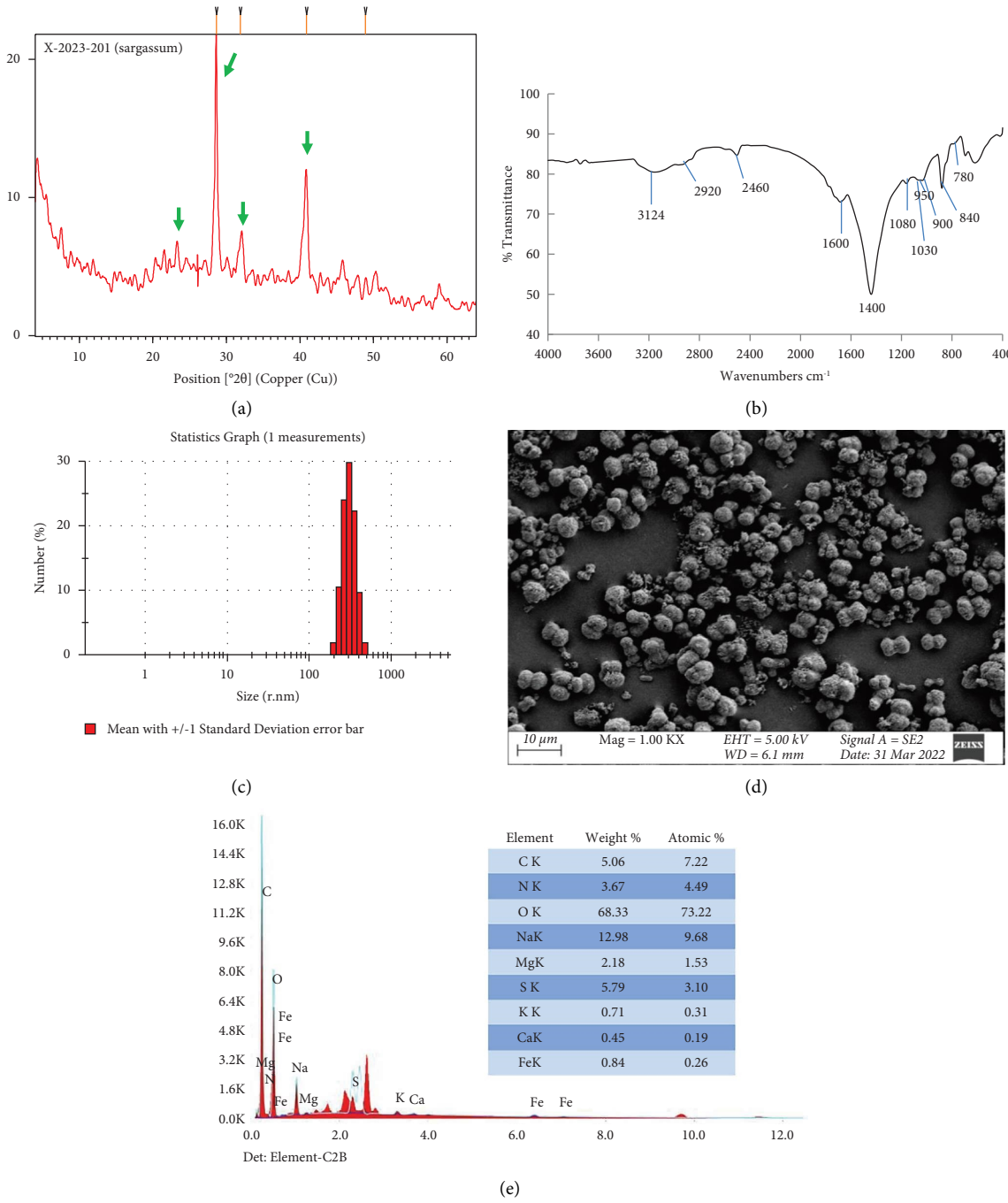

Element	Weight %	Atomic %
C K	5.06	7.22
N K	3.67	4.49
O K	68.33	73.22
NaK	12.98	9.68
MgK	2.18	1.53
S K	5.79	3.10
K K	0.71	0.31
CaK	0.45	0.19
FeK	0.84	0.26

FIGURE 7: The XRD patterns (a), FTIR spectrum (b), particle size distribution (c), FESEM picture (d), and EDX analysis (e) of the extracted alginate.

[1]. The D-mannuronate to L-guluronate ratio (M/G) can be calculated from the FTIR spectrum [101], and it has been found to be 1.01. That was comparable to *S. asperifolium* [83] and *S. latifolium* [102] alginates M/G values of 1.05. The *Sargassum* alginate M/G ratio is reported to range between 0.8 and 1.5 [103]. It has been reported that alginate with a large content of guluronic acid and a low M/G (<1) produces a strong and rigid gel [104], but elastic and soft gel are formed with alginate with a high M/G (>1) and a lower amount of guluronic acid blocks [105].

The DLS analysis (Figure 7(c)) revealed alginate with an average particle size of 311 nm. The FESEM image (Figure 7(d)) reveals rough, irregular, and spherical-shaped alginate particles with different sizes. The outer surface of alginate particles seems to have spines and perforations. A similar observation was reported for alginate extracted from *S. duplicatum* and *S. crassifolium* [96]. The EDX analysis revealed a protein content of approximately 22.94% (w/w) in the alginate extracted from *S. latifolium*. The EDX also depicted the presence of minerals: Na, Mg, Fe, Ca, and K of

6418, 2024, 1, Downloaded from https://onlinelibrary.wiley.com/doi/10.1155/2024/5184399 by Egyptian National Sci. Network (Enstinet), Wiley Online Library on [25/10/2024]. See the Terms and Conditions (https://onlinelibrary.wiley.com/terms-and-conditions) on Wiley Online Library for rules of use; OA articles are governed by the applicable Creative Commons License

approximately 12.98, 2.18, 0.84, 0.45, and 0.17% (w/w), respectively, in addition to S of approximately 5.79% (w/w). According to Mohamed et al. [86], the protein and mineral contents of alginate differ with the applied extraction methods.

The TGA/DTG plot (Figure 8(a)) matched well with that previously reported for Egyptian *S. latifolium* alginate [67]. It revealed the main thermal degradation before 100°C, which might be attributed to water evaporation [6]. The other peak, which appears at 140°C, is also reported by Nesic et al. [6], Siriwardane et al. [106], and Russo et al. [107] and was attributed to the release of bounded water, carbonate dehydration, and decomposition of protein and polyphenolic compounds, respectively. Another main thermal degradation occurred around 220°C, which, according to Nesic et al. [108], might be related to the breakdown of alginate molecules, the mannuronic blocks, followed by the guluronic blocks. The peak that appeared around 480°C might be related to the decomposition of the carbonized residue produced during the two previous main degradation stages [67].

The DSC curve (Figure 8(b)) revealed the main peak at 162.47°C, which would correspond to the melting point of alginate [109]. Xu et al. [110] reported the thermal stability of alginate up to 160°C.

3.4.3. Cellulose Yield and Characterization. The collected *S. latifolium* yielded approximately 16.40 ± 0.5% cellulose (w/w). The extracted cellulose has a purity of approximately 79.95 ± 0.05%, with hemicellulose and lignin contents of ≈0.36 ± 0.05% and 0.06 ± 0.02%, respectively.

The XRD pattern of the extracted cellulose (Figure 9(a)) was found to be well matched with that of cellulose (card number 00-003-0192) and chemical formula ($C_6H_{10}O_5$). The extracted cellulose displays the distinguished peaks of cellulose I allomorph at (2θ) 15.14°, 16.25°, 22.68°, and 34.84° (Figure 9(a), green arrows), which correspond to crystallographic planes of T10, 110, 200, and 004. This is similar to the cellulose extracted from *S. fluitans* [111] and *S. natans* [112].

The crystallinity index (CrI%) was calculated according to El-Gendy et al. [25]:

$$\mathrm{CrI}\,\% = \left(\frac{I_{200} - I_{\mathrm{amorphous}}}{I_{200}}\right) \times 100, \tag{12}$$

where the peak intensity at (2θ) 22.68° represents I_{200}, while the peak intensity at (2θ) around 18° represents the $I_{\mathrm{amorphous}}$ (Figure 9(a)). That revealed a CrI% of 93.55 ± 0.05%, confirming the high purity of the extracted crystalline cellulose [113]. That was comparable with the reported CrI% of cellulose extracted from brown *Saccharina japonica* [114] and *Sargassum vulgare* [115], which recorded 92.34% and 91.37%, respectively.

The FTIR spectrum (Figure 9(b)) shows the distinctive peaks of cellulosic polysaccharides extracted from seaweed, at 890, 1105, and 1160 cm^{-1} [113]. It matched well with the previously reported FTIR spectrum of *S. fluitans* cellulose nanocrystals [111] and *S. wightii* cellulose [61]. The peaks around 3400 and 1630 cm^{-1} are denoted for O-H stretching and bending vibrations, respectively, while the peak around 2900 cm^{-1} is consistent with the CH_2 stretching vibration. The peak appears around 1050 cm^{-1} is related to the symmetric stretching vibrations of C–O–C linkages. The peaks between 1420 cm^{-1} and 1320 cm^{-1} are related to the H–C–H scissor and H–C–H tip vibrations. The characteristic small FTIR-vibration peak of the β-glycosidic bond which is an indicative for the presence of the cellulose polymeric polysaccharides appears around 890 cm^{-1}. The absence of N-H bending vibration of lipids between 1500 cm^{-1} and 1550 cm^{-1} confirm that the extracted cellulose is free of lipid. Also, the absence of the peak around 1710 cm^{-1} of C=O indicates that the bleaching process using the hydrogen peroxide did affect the extracted cellulose and did not oxidize it or the xyloglucan [25].

The DLS analysis of the extracted cellulose (Figure 9(c)) showed a bimodal particle size distribution at 87.18 nm and 639.6 nm, with a major average particle size in the nanorange of approximately 87 nm.

The FESEM image (Figure 9(d)) revealed cellulosic fibrils. That resembles the one reported for *S. wightii* cellulose [116]. The EDX analysis (Figure 9(e)) revealed the high purity of the extracted cellulose, as it is mainly composed of carbon and oxygen with traces of minerals, and its protein content reached approximately 19.63%.

The main distinguished peak that appears in the TGA/DTG spectrum around 340°C (Figure 10(a)) might be attributed to cellulose degradation [113]. The weak peak that appears around 470°C might be related to the degradation of other secondary complexed cellulosic products, for example, cellulose esters [113]. The DSC analysis (Figure 10(b)) proved the thermal stability of the extracted cellulose, where complete decomposition would occur at ≈ 369.89°C. This increases its usefulness as a strengthening ingredient in manufacturing packaging materials and biocomposites [25].

3.5. Isolation of Fungal Strains Capable of Hydrolyzing and Saccharifying Different Algal Polysaccharides. The microbial isolation has been performed on the freshly collected *S. latifolium* biomass and its associated water. Three fungi, a yeast, and a bacterium were isolated. The three fungal isolates showed wide versatility for the utilization of algal polysaccharides (Figure 11 and Table 5), with sufficient hydrolyzing and saccharifying capabilities for the collected *S. latifolium* biomass (Table 5). The saccharification percentage ranged between 28.8 ± 0.5% and 38.52 ± 0.5%, with a corresponding TRS of approximately 1.6 ± 0. 5 g/L and 2.1 ± 0.5 g/L (Table 5). The noninoculated flasks proved the production of approximately 100 mg/L TRS. Thus, the physical hydrothermal treatment of *S. latifolium* biomass led to a saccharification % of 4.44 ± 0.09%. There was a high statistical significant difference ($p < 0.0001$) in the yielded TRS, saccharification%, and conversion% between inoculated and noninoculated flasks. That proves the efficient capabilities of the obtained fungal isolates to hydrolyze and saccharify the algal biomass. Moreover, there was a high statistical significant difference ($p < 0.0001$) in the yielded

6418, 2024, 1, Downloaded from https://onlinelibrary.wiley.com/doi/10.1155/2024/5184399 by Egyptian National Sci. Network (Enstinet), Wiley Online Library on [25/10/2024]. See the Terms and Conditions (https://onlinelibrary.wiley.com/terms-and-conditions) on Wiley Online Library for rules of use; OA articles are governed by the applicable Creative Commons License

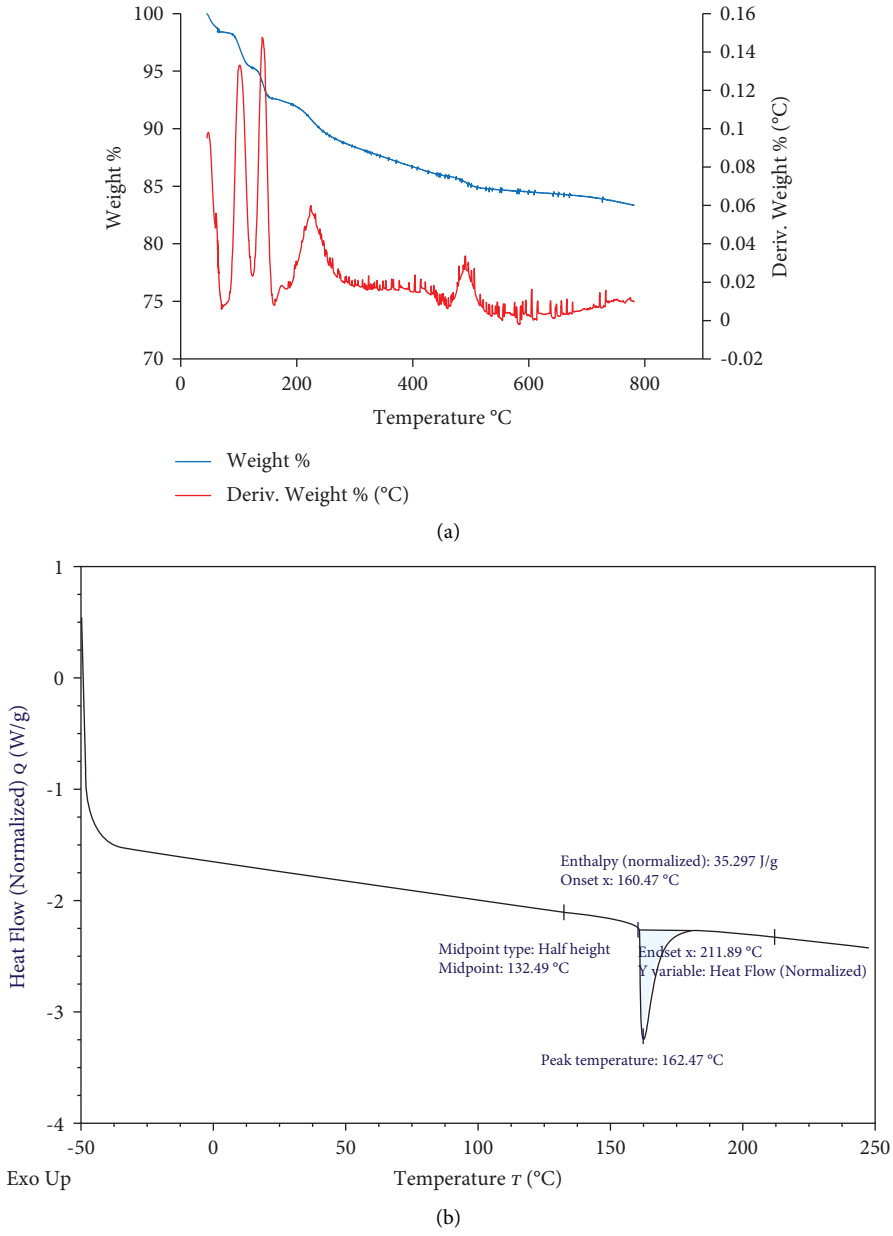

Figure 8: TGA/DTG (a) and DSC (b) analyses of the extracted alginate.

TRS, saccharification%, and conversion% performed by *P. oxalicum* SBWF3 relative to those *A. galapagensis* SBWF1 and *M. hiemalis* SBWF2. However, there is a relatively statistical significant difference ($p < 0.0069$) between the performance of SBWF1 and BWF2.

The obtained fungal isolates were identified as *Aspergillus galapagensis* strain SBWF1 (GenBank accession number OR636487), *Mucor hiemalis* strain SBWF2 (GenBank accession number OR636488), and *Penicillium oxalicum* strain SBWF3 (GenBank accession number OR636489). Their phylogenetic trees are illustrated in Figure 12.

Typically, costly enzymes are used to complete the hydrolysis or saccharification of acid-hydrolyzed macroalgae [47, 59, 117]. However, the produced TRS yield in this study using the eco-friendly hydrothermal pretreatment and the intact fungus as an enzymatic source showed to be very promising and ranged between approximately 317.48 ± 1.75 and 428.62 ± 1.5 mg TRS/g *S. latifolium* biomass (Table 5). That was higher than those reported by Soliman et al. [12], where *A. niger* HN3 and *Penicillium* sp. HN1 yielded 136.4 and 109 mg TRS/g *S. latifolium* biomass, respectively. Moreover, the recorded conversion% $31.75 \pm 0.2\%$–$42.86 \pm 0.2\%$ (Table 5) were much higher than those reported by Kooren et al. [13] applying different costly physical and chemical saccharification processes to *S. wightii* biomass, which ranged between 9.33% and 18.67%. Thus, the obtained fungal strains overcome the presence of alginate, which is one of the main obstacles to bioethanol production [118].

6418, 2024, 1, Downloaded from https://onlinelibrary.wiley.com/doi/10.1155/2024/5184399 by Egyptian National Sci. Network (Enstinet), Wiley Online Library on [25/10/2024]. See the Terms and Conditions (https://onlinelibrary.wiley.com/terms-and-conditions) on Wiley Online Library for rules of use; OA articles are governed by the applicable Creative Commons License

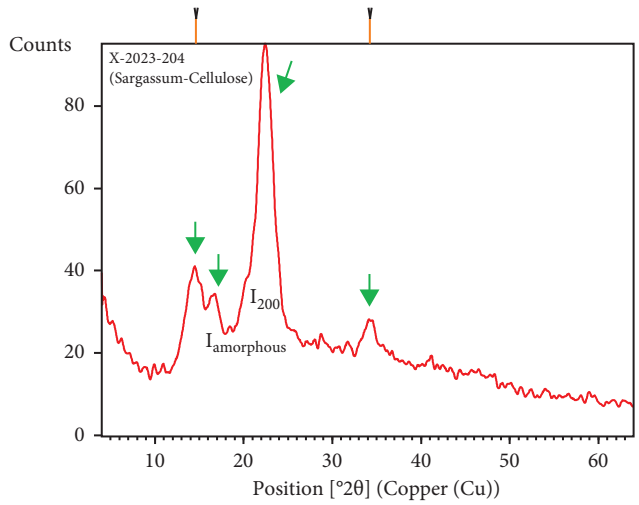

(a)

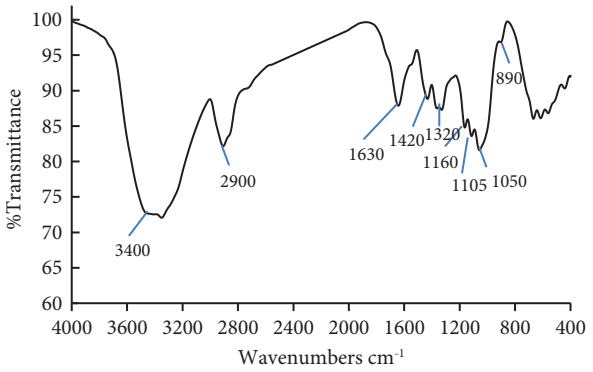

(b)

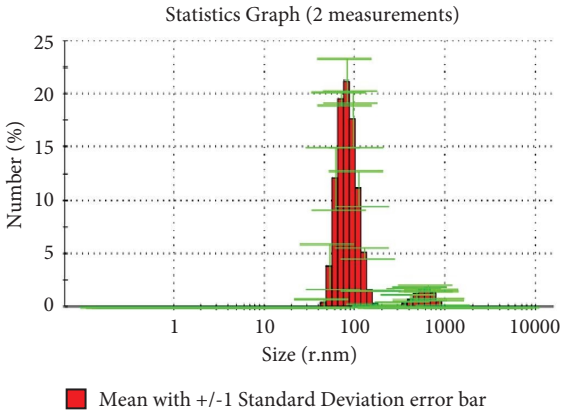

(c)

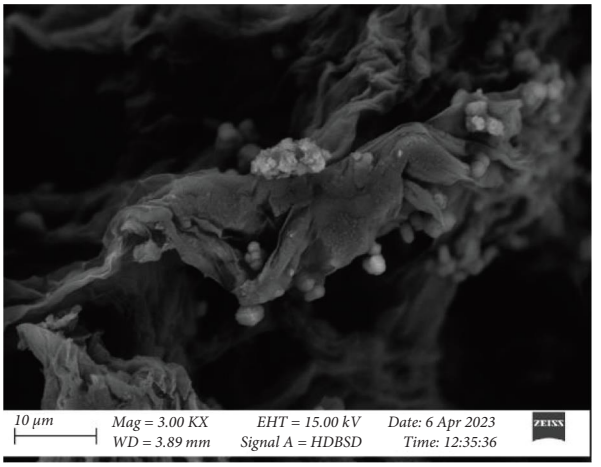

(d)

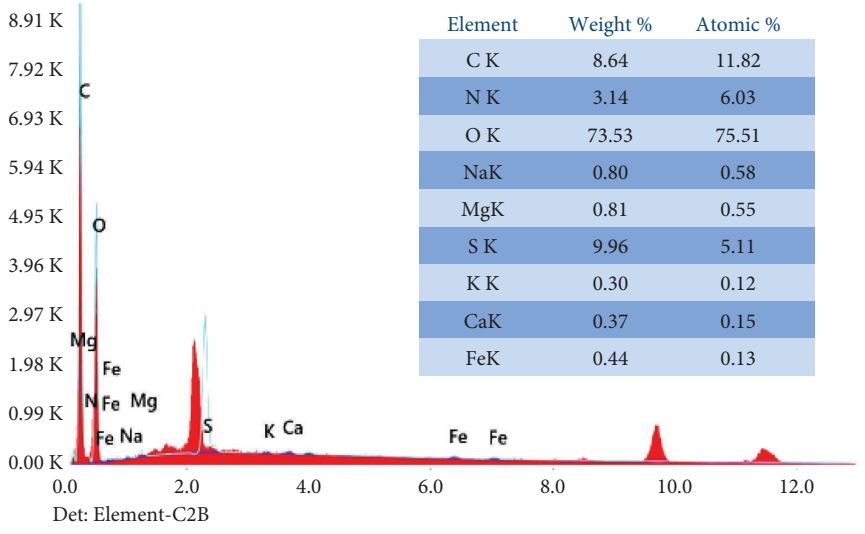

Element	Weight %	Atomic %
C K	8.64	11.82
N K	3.14	6.03
O K	73.53	75.51
NaK	0.80	0.58
MgK	0.81	0.55
S K	9.96	5.11
K K	0.30	0.12
CaK	0.37	0.15
FeK	0.44	0.13

(e)

Figure 9: The XRD patterns (a), FTIR spectrum (b), particle size distribution (c), FESEM picture (d), and EDX analysis (e) of the extracted cellulose.

6418, 2024, 1, Downloaded from https://onlinelibrary.wiley.com/doi/10.1155/2024/5184399 by Egyptian National Sci. Network (Enstinet), Wiley Online Library on [25/10/2024]. See the Terms and Conditions (https://onlinelibrary.wiley.com/terms-and-conditions) on Wiley Online Library for rules of use; OA articles are governed by the applicable Creative Commons License

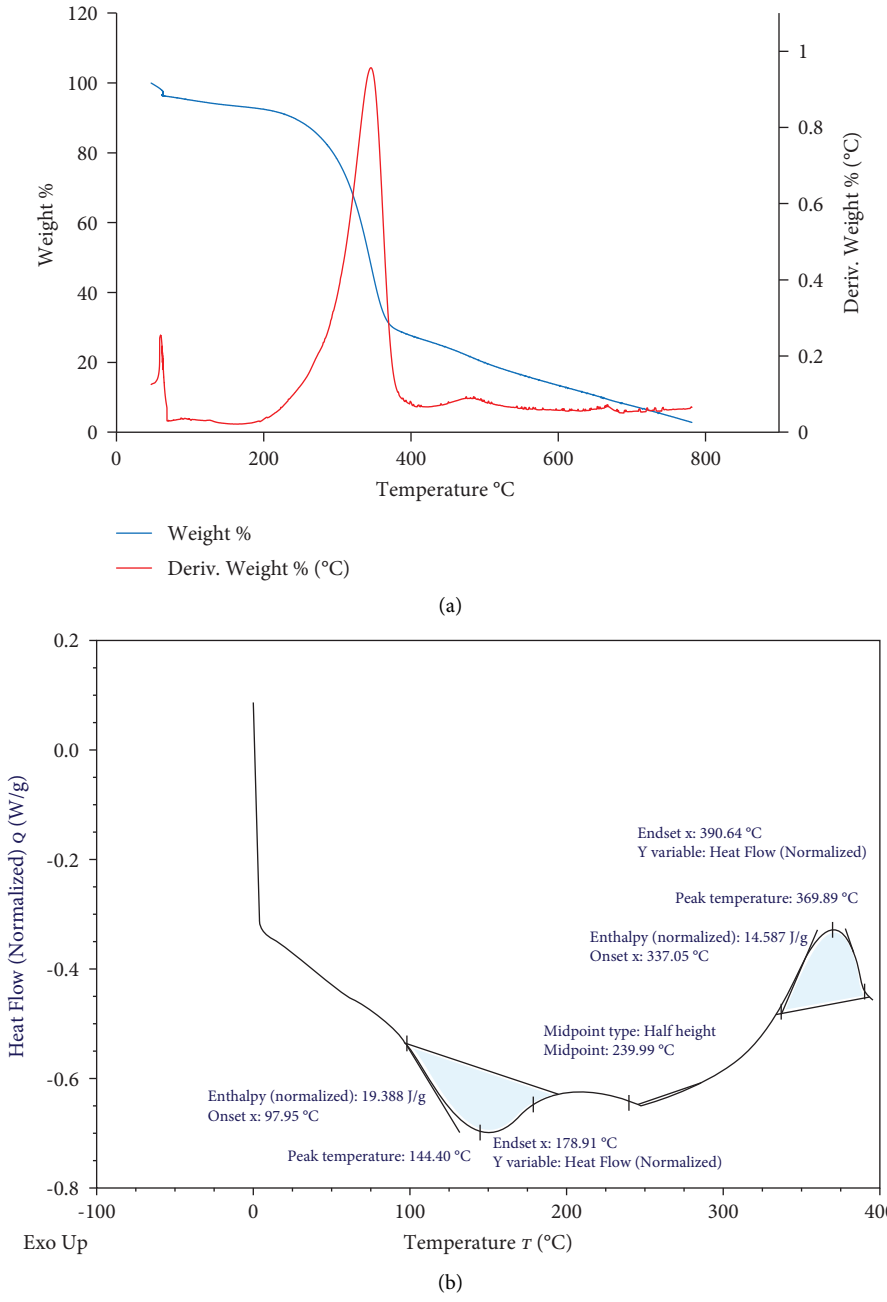

Figure 10: TGA/DTG (a) and DSC (b) analyses of the extracted cellulose.

3.6. Isolation of Microbial Isolates Capable of Fermenting Different Di- and Monosaccharides. There was no detected bioethanol production or sugar decrease in noninoculated flasks (−ve control). According to the data listed in Tables 6 and 7, the isolated bacteria and yeast showed good capabilities for fermenting pentoses, hexoses, and mannitol into bioethanol. They were identified as *Stutzerimonas stutzeri* strain SBB1 (GenBank accession number OR764547) and *Candida tropicalis* strain SBY1 (GenBank accession number OR636490), respectively. Their phylogenetic trees are illustrated in Figure 13. *C. tropicalis* KCTC7212 has been previously reported for fermenting mannitol into bioethanol [119]. *C. tropicalis* has been previously isolated from the Egyptian Red Sea for the utilization of seaweed for bioethanol production [120]. The marine bacterium *Pseudomonas stutzeri*, which is now known as *Stutzerimonas stutzeri* [121], has been isolated for bioethanol production from seaweed [11, 122].

It can be depicted from data listed in Table 7, that there was a high statistical significant difference ($p < 0.0001$) in the bioethanol fermentation capabilities of *S. stutzeri* SBB1 and *C. tropicalis* SBY1, yielding 0.73 ± 0.029 and 0.39 ± 0.014 g bioethanol/g algae, respectively. Moreover, SBB1 showed higher capabilities for utilization of mannitol and xylose than SBY1 ($p < 0.0001$), with nearly the same capabilities of utilizing glucose ($p > 0.05$). Thus, *S. stutzeri* SBB1 is

6418, 2024, 1, Downloaded from https://onlinelibrary.wiley.com/doi/10.1155/2024/5184399 by Egyptian National Sci. Network (Enstinet), Wiley Online Library on [25/10/2024]. See the Terms and Conditions (https://onlinelibrary.wiley.com/terms-and-conditions) on Wiley Online Library for rules of use; OA articles are governed by the applicable Creative Commons License

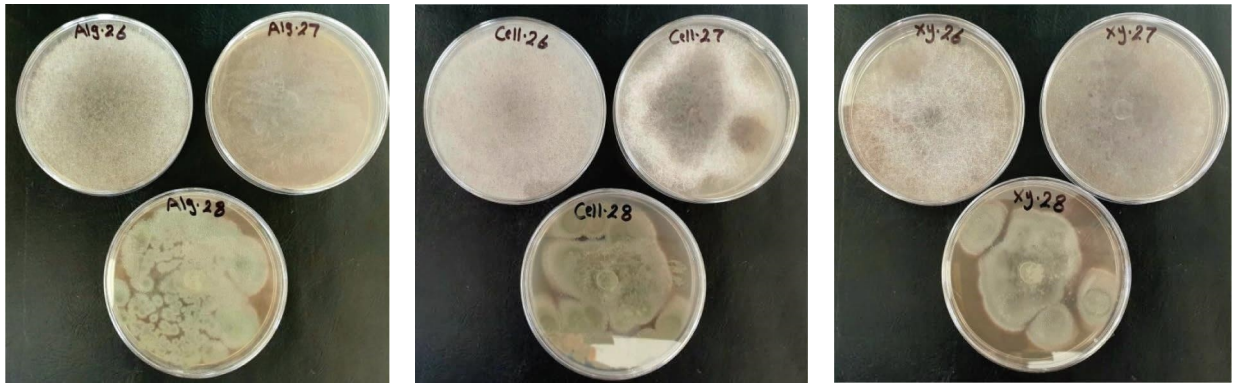

(a) (b) (c)

Figure 11: Growth of fungal isolates on different algal polysaccharides: (a) alginate plates, (b) cellulose plates, and (c) Xylan plates.

Table 5: The performance of fungal isolates on different polysaccharides and algal biomass.

Fungal code	Fungal isolate	Growth efficiency on different algal polysaccharides			
26	*A. galapagensis* SBWF1	Alginate ≈ cellulose ≈ xylan			
27	*M. hiemalis* SBWF2	Cellulose ≈ xylan > alginate			
28	*P. oxalicum* SBWF3	Alginate ≈ cellulose ≈ xylan			
	Hydrolysis and saccharification of *S. latifolium* biomass by the obtained fungal isolates				
Fungal code	Fungal isolate	Produced TRS mg/L	Yield mg/g	Saccharification %	Conversion %
26	*A. galapagensis* SBWF1	1587.4 ± 2.43	317.48 ± 1.75	70.55 ± 0.11	31.75 ± 0.17
27	*M. hiemalis* SBWF2	1684.22 ± 2.98	336.84 ± 1.3	74.85 ± 0.14	33.68 ± 0.13
28	*P. oxalicum* SBWF3	2141.55 ± 2.20	428.62 ± 1.5	95.18 ± 0.10	42.86 ± 0.15
	−ve control	100 ± 2.00	20 ± 0.5	4.44 ± 0.09	2 ± 0.05

recommendable to overcome the second main obstacle of bioethanol production from brown macroalgae, and it has further been tested for fermenting the obtained algal hydrolyzates. That produced a sufficient bioethanol yield of approximately 0.25 ± 0.014, 0.26 ± 0.018, and 0.37 ± 0.020 g ethanol/g algal biomass, with a corresponding actual bioethanol yield of 0.79 ± 0.007, 0.77 ± 0.007, and 0.86 ± 0.007 g ethanol/g TRS, from the hydolyzates obtained from SSF using *A. galapagensis* SBWF1, M. *hiemalis* SBWF2, and *P. oxalicum* SBWF3, respectively (Table 7). It is worth mentioning that there was no statistical significant different between the bioethanol yields obtained from the SBWF1 and SBWF2 hydrolyzates ($p > 0.05$). Yet, there is a statistical significant difference between the yielded bioethanol from SBWF3 hydrolyzate and the other aforementioned SBWF1 and SBWF2 hydrolyzates (p0.001). The tabulated bioethanol yields (Table 7) were higher than those reported for acid and enzymatic hydrolysis of *S. horneri*, followed by fermentation using *Pichia stipitis*, which yielded 0.11 g ethanol/g algal biomass [46]. These were also higher than the actual bioethanol yield reported by Kadimpati et al. [123] for the acid hydrolysis of *S. cinereum*, followed by fermentation using *Saccharomyces cerevisiae* MTCC170, which yielded 0.465 g ethanol/g TRS. Those were also higher than that reported by Soliman et al. [12] for hydrothermal and fungal hydrolysis and saccharification of *S. latifolium* by SSF using *Trichoderma asperellum* RM1, followed by fermentation using a consortium of two *Saccharomyces cerevisiae* strains, ATCC 76621 and RM2, which yielded 0.29 ethanol/g TRS.

The recorded bioethanol conversion yields of *A. galapagensis* SBWF1 and *M. hiemalis* SBWF2 hydrolyzates of 79 ± 0.70% and 77 ± 0.70%, respectively (Table 7), were comparable to those reported for hydrothermal and enzymatic hydrolysis of *Sargassum* species, followed by fermentation using *Saccharomyces cerevisiae* PE-2, which yielded 76.23% of bioethanol conversion [48]. Nevertheless, the recorded bioethanol conversion yield of *P. oxalicum* SBWF3 hydrolyzate of 86 ± 0.70% (Table 7) was comparable to that reported for acid and enzymatic hydrolysis of *Sargassum* species followed by fermentation using *Saccharomyces cerevisiae*, which yielded 89% of bioethanol conversion [59].

Table 7 shows that the recorded bioethanol conversion yields exceeded the theoretical yield associated with glucose, which is 51%. That might be due to the presence of other fermentable sugars (Figure 14), which would have been fermented to ethanol after the complete consumption of glucose [124]. The sugars' profiles of the three hydrolyzates before and after the bioethanol fermentation process (Figure 14) confirmed the wide versatility of *S. stutzeri* SBB1 for utilizing reducing hexoses and pentoses, nonreducing sucrose, and mannitol.

6418, 2024, 1, Downloaded from https://onlinelibrary.wiley.com/doi/10.1155/2024/5184399 by Egyptian National Sci. Network (Enstinet), Wiley Online Library on [25/10/2024]. See the Terms and Conditions (https://onlinelibrary.wiley.com/terms-and-conditions) on Wiley Online Library for rules of use; OA articles are governed by the applicable Creative Commons License

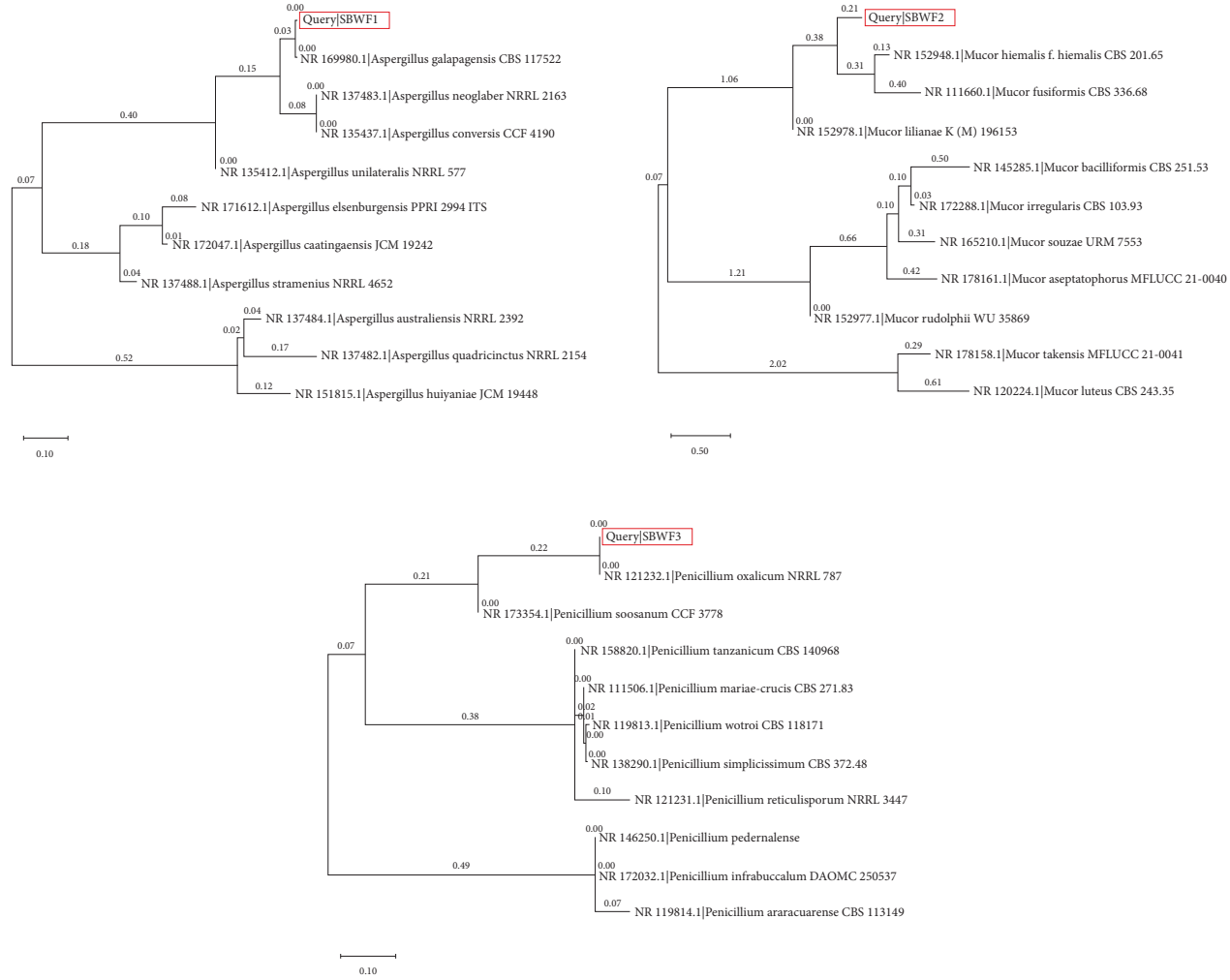

Figure 12: Maximum likelihood phylogenetic trees for ITS regions of three fungal isolates.

Table 6: The capacities of the bacterial and yeast isolates to utilize different sugars.

Microbial isolates	Mannitol	Lactose	Sucrose	Xylose	Mannose	Fructose	Maltose	Galactose	Glucose	Arabinose
C. tropicalis SBY1	++	++	++	++	++	++	++	++	++	++
S. stutzeri SBB1	++	++	+++	+++	+++	+++	+++	+++	+++	+++

Elshobary et al. [125] stated that multiplying the produced amount of bioethanol (g/g biomass) by the corresponding calorific value of 26.7 MJ/kg will give an estimate of the energy output based on the estimated energy stored in the bioethanol. Thus, based on the data listed in Table 7, the energy output was estimated to be approximately 6.68 ± 0.37, 6.94 ± 0.22, and 9.88 ± 0.53 MJ/kg for bioethanol yields of *A. galapagensis* SBWF1, *Mucor hiemalis* SBWF2, and *P. oxalicum* SBWF3 hydrolyzates, respectively. It is noteworthy to emphasize the high statistical significant difference ($p < 0.0001$) between the energy output for bioethanol yield of *P. oxalicum* SBWF3 hydrolyzate relative to those of SBWF1 and SBWF1, besides the nonstatistical significant difference between those of SBWF1 and SBWF1 ($p > 0.05$). Thus, the suggested solid state fungal hydrolysis and saccharification of using *P. oxalicum* SBWF3 that sequentially followed by a separate fermentation process using *S. stutzeri* SBB1 would be recommendable for further industrial scale studies.

3.7. The Macroalgal Synthesis of Carbon-Dot (CD). The green synthesis of the CD was done using the aqueous extract of spent waste biomass of *S. latifolium*, disposed of from the bioethanol production process, without using any chemical oxidizing agents. The obtained clear yellowish suspension of CD displayed strong bright green fluorescence under UV light-λ_{365nm} (Figure 15(a)). Mewada et al. [126] reported a similar observation. That suggests its suitability for being used in cellular imaging [126]. According to

6418, 2024, 1, Downloaded from https://onlinelibrary.wiley.com/doi/10.1155/2024/5184399 by Egyptian National Sci. Network (Enstinet), Wiley Online Library on [25/10/2024]. See the Terms and Conditions (https://onlinelibrary.wiley.com/terms-and-conditions) on Wiley Online Library for rules of use; OA articles are governed by the applicable Creative Commons License

Table 7: The fermentation capabilities of the isolated bacteria and yeast.

Microbial isolates	Fermentation capabilities on a mixture of standard sugars				
	Residual sugars mg/L			Bioethanol g/L	Bioethanol yield g ethanol/g sugars
	Glucose	Xylose	Mannitol		
−ve control	2000	2000	2000	Nil	Nil
C. tropicalis SBY1	3	1343	1550	2.33 ± 0.035	0.39 ± 0.014
S. stutzeri SBB1	2	333	125	4.38 ± 0.212	0.73 ± 0.029
Fungal hydrolyzates	Bioethanol production from *S. latifolium* by *Stutzerimonas stutzeri* strain SBB1				
	Produced TRS mg/L	Bioethanol g/L	Actual bioethanol yield g ethanol/g TRS	Bioethanol conversion yield	Bioethanol yield g ethanol/g algal biomass
A. galapagensis SBWF1	1587.4 ± 0.43	1.25 ± 0.035	0.79 ± 0.007	79%±0.70	0.25 ± 0.014
M. hiemalis SBWF2	1682.11 ± 2.98	1.30 ± 0.014	0.77 ± 0.007	77%±0.70	0.26 ± 0.018
P. oxalicum SBWF3	2141.55 ± 2.2	1.85 ± 0.048	0.86 ± 0.007	86%±0.70	0.37 ± 0.020

6418, 2024, 1, Downloaded from https://onlinelibrary.wiley.com/doi/10.1155/2024/5184399 by Egyptian National Sci. Network (Enstinet), Wiley Online Library on [25/10/2024]. See the Terms and Conditions (https://onlinelibrary.wiley.com/terms-and-conditions) on Wiley Online Library for rules of use; OA articles are governed by the applicable Creative Commons License

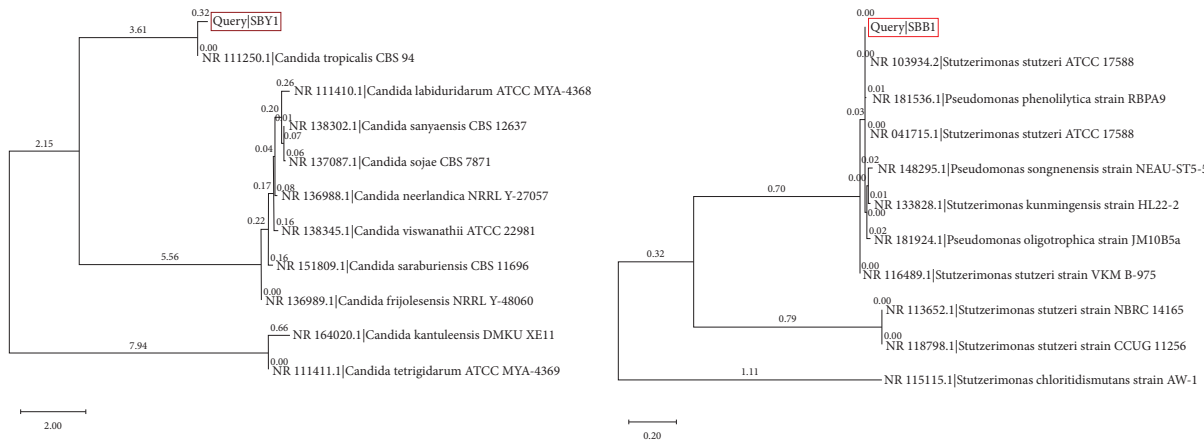

Figure 13: Maximum likelihood phylogenetic tree for the ITS regions of yeast isolate SBY1 (a) and for the 16S rDNA region of isolate SBB1 (b).

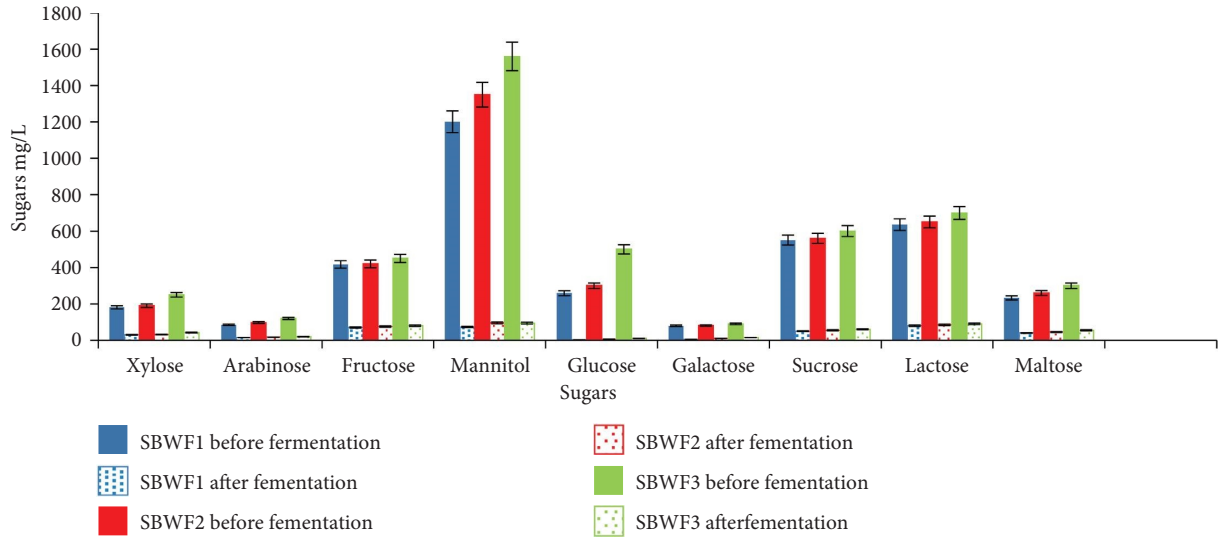

Figure 14: Sugar profile of the obtained *S. latifolium* hydrolyzates before and after bioethanol fermentation process.

Mewada et al. [126], the recombination of electron-hole pairs from impurity atoms and oxygen-bearing functional groups may be the reason for the CD-fluorescence. The EDX analysis revealed the presence of O, Na, and N, besides C, of approximately $33.76 \pm 0.05\%$, $7.28 \pm 0.05\%$, $4.24 \pm 0.05\%$, and $54.72 \pm 0.05\%$ (w/w), respectively, which coincides with the previously reported EDX of green-synthesized CD using *Osmanthus fragrans* flowers [127].

The PL spectrum of the *S. latifolium*-synthesized CD (Figure 15(a)) recorded maximum emission intensity at 520 nm, which matches that reported by Bhattacharya et al. [128].

The Raman spectrum (Figure 15(b)) depicts one main sharp band (1365 cm^{-1}), which expresses the D-band. The predominance of D-band over G-band has been previously reported for the green-synthesized CD and indicates functionalized CD with an unassertive graphitic structure [129, 130]. Primarily, D- and G-bands are linked with the vibrational form of sp^3 and sp^2 hybridized carbon atoms and denoted for disorder and graphitic band, respectively [130].

The FESEM (Figure 15(c)) and HRTEM (Figure 15(d)) analyses proved the predominance of monodispersed spherical-shaped CS with a narrow average size distribution ranging between 11 nm and 15 nm. According to Hoan et al. [131] and Eskalen et al. [132], the apparent mesh structures of CD in the HRTEM image (Figure 15(d)) would indicate amorphous CD.

The FTIR spectrum (Figure 15(e)) shows an absorption band at 2800 cm^{-1}, which can be assigned to -C-H stretching of the methyl or methylene groups associated with the aliphatic hydrocarbons present in the *S. latifolium* extract. The two bands at 3843 cm^{-1} and 3745 cm^{-1} might be due to the O-H stretching of phenolic -OH and -COOH, respectively. The peak around 3430 cm^{-1} might be related to the -NH of amine groups in the *S. latifolium* aqueous extract.

6418, 2024, 1, Downloaded from https://onlinelibrary.wiley.com/doi/10.1155/2024/5184399 by Egyptian National Sci. Network (Enstinet), Wiley Online Library on [25/10/2024]. See the Terms and Conditions (https://onlinelibrary.wiley.com/terms-and-conditions) on Wiley Online Library for rules of use; OA articles are governed by the applicable Creative Commons License

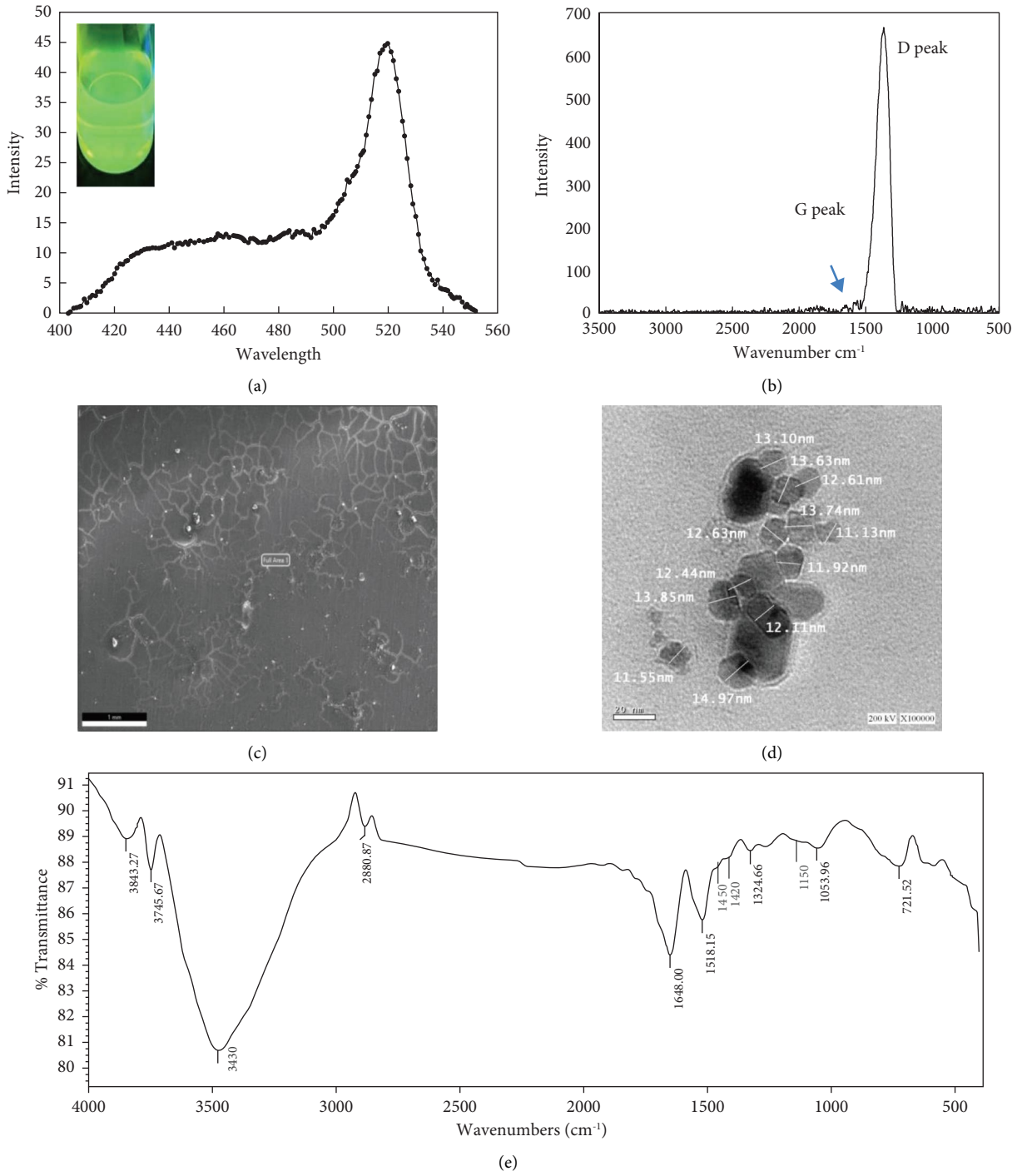

FIGURE 15: PL spectrum (a), Raman spectrum (b), FESEM image (c), HRTEM image (d), and FTIR spectrum (e) of the algal-synthesized C-dots.

The absorption band at 1648 cm^{-1} is due to -C=O, while the vibrational band of -COOH appears around 1324 cm^{-1}. The vibrational bands of–C-N and N-OH appear around 1450 cm^{-1} and 1425 cm^{-1}, respectively. The peak at 1518 cm^{-1} might be related to -C=C- stretching of aromatics.

The peak around 1053 cm^{-1} might be related to the -C-O-C- linkages, while the peak around 1150 cm^{-1} might be attributed to the stretching band of C-N. The aforementioned functional groups would confirm the carbon dots with aqueous-soluble nature [126]. The FTIR analysis confirmed the EDX analysis, and according to Wu et al. [133] and Lai et al. [134], the presence of the hydrophilic amino, carbonyl, and hydroxyl functional groups enhances the CD water solubility. Moreover, according to Mewada et al. [126], the presence of methyl and hydroxyl groups in CD is also advantageous, as they can serve as

6418, 2024, 1, Downloaded from https://onlinelibrary.wiley.com/doi/10.1155/2024/5184399 by Egyptian National Sci. Network (Enstinet), Wiley Online Library on [25/10/2024]. See the Terms and Conditions (https://onlinelibrary.wiley.com/terms-and-conditions) on Wiley Online Library for rules of use; OA articles are governed by the applicable Creative Commons License

Table 8: The antimicrobial activity of the algal-synthesized C-dot.

Compound ID	Tested microorganisms					
	B. subtilis ATCC 6633	*S. aureus* ATCC 35556	*E. coli* ATCC 23282	*P. putida* ATCC 10145	*C. albicans* IMRU 3669	*A. niger* ATCC 16404
C-dot	25 ± 0.45	23 ± 0.36	17 ± 0.29	27 ± 0.48	28 ± 0.35	25 ± 0.29
Reference antibiotic	32 ± 0.7	34 ± 0.7	24 ± 0.44	30 ± 0.66	21 ± 0.52	22 ± 0.44
Activity index	0.78 ± 0.02	0.68 ± 0.07	0.71 ± 0.03	0.9 ± 0.01	1.33 ± 0.02	1.14 ± 0.01

linkers for the attachment of therapeutic moieties, such as medications, for specific delivery to diseased cells.

The green-synthesized CD proved to have efficient biocidal activity against different pathogenic microorganisms (Table 8). It expressed higher biocidal activity against the pathogenic fungus *Aspergillus niger* ATCC 16404 and the yeast *Candida albicans* IMRU 3669, relative to the standard metronidazole (100 μg/mL). It recorded an activity index of approximately 1.14 ± 0.01 and 1.33 ± 0.02, with a statistical significant difference from the reference antibiotic of $p = 0.001$ and $p = 0.0005$, at the 95% confidence level, respectively. It is worth mentioning that its activity index against the studied pathogenic fungus and yeast strains is statistically higher than that recorded against the studied pathogenic Gram-positive and Gram-negative bacteria ($p < 0.0001$). Yet, it is still expressing a sufficient biocidal activity against the studied Gram-positive and Gram-negative pathogenic bacteria as compared to the standard antibiotic streptomycin (50 μg/mL). The green-synthesized CD showed a statistically higher biocidal activity on the Gram-negative *Pseudomonas putida* ATCC 10145 relative to that on *Escherichia coli* ATCC 23282 ($p < 0.0001$). Nevertheless, it recorded an activity index of approximately 0.9 ± 0.01 and 0.71 ± 0.03, with a statistical significant difference from the reference antibiotic of $p = 0.001$ and $p = 0.0003$, at the 95% confidence level, respectively. The green-synthesized C-dot expressed a slightly higher biocidal activity against the pathogenic Gram-positive *Bacillus subtilis* ATCC 6633 than that expressed against the pathogenic Gram-positive *Staphylococcus aureus* ATCC 35556 ($p = 0.001$). That recorded a corresponding activity index of approximately 0.78 ± 0.02 and 0.68 ± 0.07, with a statistical significant difference from the reference antibiotic of $p = 0.0007$ and $p = 0.0002$, at the 95% confidence level, respectively. The tabulated antimicrobial efficiency of *S. latifolium* CD (Table 8) is better than that reported for pomegranate peel-based CD [135].

The antimicrobial activity of CD has been previously reported by Dong et al. [136], and it is attributed to the formation of reactive oxygen species (ROS), leading to disruption in bacterial cell walls, damaging the protein, RNA, and DNA, inhibiting some gene expressions, causing leakage of the cytoplasmic contents, and cellular inactivation [137, 138]. However, to the best of our knowledge, it is the first record for the biocidal activity of seaweed-based carbon-dot.

3.8. The Attained Valued Merchandises and Their Recommended Conceivable Uses. The main obstacle in utilizing brown macroalgae for the production of bioethanol is the presence of mannitol and alginate. However, this research overcomes such an obstacle by isolating fungal strains capable of hydrolyzing and saccharifying different polysaccharides of *Sargassum latifolium*, in addition to bacteria capable of fermenting pentoses, hexoses, and mannitol. Those yielded approximately 0.32 ± 0.002–0.43 ± 0.002 g fermentable sugars/g algal biomass and 0.25 ± 0.014–0.37 ± 0.02 g ethanol/g algal biomass, respectively. Further work is undergoing now for optimization of the fungal hydrolysis and saccharification of *S. Latifolium* and bioethanol fermentation processes using the obtained microbial isolates to maximize the yield of fermentable sugars and bioethanol.

S. Latifolium is found to be an excellent source of natural pigments, antioxidants, carbohydrates, lipids, proteins, fibers, and inorganic minerals, as well as other valuable biopolymers, which are alginate and cellulose. This recommends the implementation of worthwhile biorefinery for green and sustainable products based on marine brown macroalgal biomass (for example, *S. Latifolium*). That would consequently create a new market for the clean and sustainable bio-based blue economy in Egypt, which is expected to be very promising and strategic as macroalgae, its main feedstock, require only carbon dioxide, sunlight, and seawater for growth and proliferation. Moreover, the *S. latifolium* biomass itself can be applied for the production of solid and liquid biofuels. It can also be used in the organic fertilizers and animal fodder industries. Furthermore, it acts as a source of pure alginate, which can be used as stabilizers in the food, beverage, pharmaceutical, and textile industries. Alginate can also be applied for mulching, wastewater treatment, and in many bioprocesses and biomedical applications. It can be used in biofuels, paper, pharmaceutical, and food industries due to its cellulose content.

In addition, the suggested solid-state fungal hydrolysis and saccharification followed by separate bioethanol fermentation and the fully integrated process for extraction of value-added products are completely green and sustainable and do not require any toxic chemicals. They use less energy and water, produce fewer waste effluents, and run under mild operating conditions. Furthermore, the advocated valorization of the spent waste *S. latifolium* into the C-dot

6418, 2024, 1, Downloaded from https://onlinelibrary.wiley.com/doi/10.1155/2024/5184399 by Egyptian National Sci. Network (Enstinet), Wiley Online Library on [25/10/2024]. See the Terms and Conditions (https://onlinelibrary.wiley.com/terms-and-conditions) on Wiley Online Library for rules of use; OA articles are governed by the applicable Creative Commons License

would also lower the process waste, decrease the overall cost of the process, and make it more feasible. Since the C-dot has many applications in forensics, imaging, sensors, herbicide detection, heavy metal detection, drug delivery, antioxidants, photocatalysis, optoelectronics, and biocides against pathogenic microorganisms.

Therefore, rather than being viewed as polluting waste, *S. latifolium* can be considered a resource for cleaner production, leading to a net reduction in emissions and enrichment in the industrial sector and economy. Yet, it is worth knowing that the exact cost of *S. Latifolium*-derived merchandise is not yet recognized, and large-scale economic analysis is currently under investigation. However, the results of this study reduce the detrimental effects of harmful macroalgal blooms and beach piles on tourism, the environment, and the economy by maximizing biomass conversion and preventing the spread of invasive macroalgal biomass along the Egyptian Red Sea shorelines.

4. Conclusion

This study showed that the readily available massively proliferated brown macroalgae along the Egyptian Red Sea shorelines, *Sargassum latifolium*, which causes eutrophication problems, damages and deteriorates coral reefs, negatively affects aquatic ecosystems and biodiversity, and harms shorelines, can operate as a win-win key along the entire production chain process for a number of energy, industrial, environmental, and economic challenges. Nevertheless, much more research is required to evaluate the commercial and practical viability of the advocated blue-based technology. This is because a lot of variables will affect it, such as the harvesting season and costs, sustainability and feedstock processing, product marketability, and how well they work in other low-carbon footprint industries.

Data Availability

Data are available from the corresponding author upon request.

Disclosure

We have followed our ethical norms established by our respective institutions.

Conflicts of Interest

The authors declare that they have no conflicts of interest.

Authors' Contributions

N.Sh.E.-G. put forth the idea of scientific research, conceived and designed research, supervised experimental work, validated the results, interpreted and discussed the results, and wrote the manuscript; M.H. performed collection and sampling of macroalgae, isolation of microbial isolates capable of hydrolyzing and saccharifying brown seaweeds and fermenting produced pentoses, hexoses, mannitol, and disaccharides into bioethanol, in addition to all bioethanol part; A.R.I. conceived the biocidal tests of the green-synthesized C-dots, all analysis of the value-added products, and participated in the identification and preservation of the microbial isolates; A.A.R. performed all the genetic identification of the obtained microbial isolates; H.R.A. and B.A.A. performed all the extraction and analysis of the value-added products; R.A.E.-S. green synthesis of C-dots and its full characterization; K.M.A. performed the microscopic identification of macroalgae; M.M. performed all physicochemical analyses of macroalgae. All authors have read and agreed to the published version of the manuscript. We declare that all authors of this manuscript have made substantial contributions. We have not excluded any author that substantially contributed to this manuscript.

Acknowledgments

The authors express their gratitude to the Science, Technology and Innovation Funding Authority (STDF) for funding this work under the grand number (45614).

References

[1] S. H. Rashedy, M. S. M. Abd ElHafez, M. A. Dar, J. Cotas, and L. Pereira, "Evaluation and characterization of alginate extracted from brown seaweed collected in the Red Sea," *Applied Sciences*, vol. 11, p. 6290, 2021.

[2] N. M. S. Moubayed, H. J. Al Houri, M. M. Al Khulaifi, and D. A. Al Farraj, "Antimicrobial, antioxidant properties and chemical composition of seaweeds collected from Saudi Arabia (Red Sea and Arabian Gulf)," *Saudi Journal of Biological Sciences*, vol. 24, no. 1, pp. 162–169, 2017.

[3] S. E. Abu Ahmed, M. A. Deyab, N. I. Hassan, and M. M. El-Sheekh, "Physicochemical characterization of Sargassum latifolium at Ras Sudr shores—red sea coast of Egypt. Egypt," *Journal de Botanique, Le*, vol. 62, no. 3, pp. 763–776, 2022.

[4] G. A. Ismail, M. Hessien, M. A. Saleh, and M. M. Ismail, "Antioxidant and antiviral activity of sulfated polysaccharides derived from two *Sargassum* species of Red Sea Egypt," *Journal of Biologically Active Products from Nature*, vol. 12, no. 4, pp. 324–343, 2022.

[5] M. Wang, C. Hu, B. B. Barnes, G. Mitchum, B. Lapointe, and J. P. Montoya, "The great Atlantic *Sargassum* belt," *Science*, vol. 365, no. 6448, pp. 83–87, 2019.

[6] A. Nesic, M. V. De Bonis, G. Dal Poggetto, G. Ruocco, and G. Santagata, "Microwave assisted extraction of raw alginate as a sustainable and cost-effective method to treat beach-accumulated *Sargassum* algae," *Polymers*, vol. 15, no. 14, p. 2979, 2023.

[7] R. E. Rodríguez-Martínez, A. E. Medina-Valmaseda, P. Blanchon et al., "Faunal mortality associated with massive beaching and decomposition of pelagic *Sargassum*," *Marine Pollution Bulletin*, vol. 146, pp. 201–205, 2019.

[8] B. I. van Tussenbroek, H. A. Hernández Arana, R. E. Rodríguez-Martínez et al., "Severe impacts of brown tides caused by *Sargassum* spp. on near-shore Caribbean seagrass communities," *Marine Pollution Bulletin*, vol. 122, no. 1-2, pp. 272–281, 2017.

[9] A. S. Maurer, E. De Neef, and S. Stapleton, "*Sargassum* accumulation may spell trouble for nesting sea turtles," *Frontiers in Ecology and the Environment*, vol. 13, no. 7, pp. 394-395, 2015.

6418, 2024, 1, Downloaded from https://onlinelibrary.wiley.com/doi/10.1155/2024/5184399 by Egyptian National Sci. Network (Enstinet), Wiley Online Library on [25/10/2024]. See the Terms and Conditions (https://onlinelibrary.wiley.com/terms-and-conditions) on Wiley Online Library for rules of use; OA articles are governed by the applicable Creative Commons License

[10] M.-C. Lee, H.-Y. Yeh, C.-M. Chang, Y.-F. Liou, F.-H. Nan, and J. Wungen-Sani, "Tracking and utilizing Sargassum, an abundant resource from the caribbean sea," *Water*, vol. 15, p. 2694, 2023.

[11] B. R. Mohapatra, "Fermentation medium optimization, molecular modelling and docking analysis of the alginate lyase of a novel *Pseudomonas* sp. LB56 isolated from seaweed waste," *Biotechnology and Biotechnological Equipment*, vol. 36, no. 1, pp. 281–291, 2022.

[12] R. M. Soliman, S. A. Younis, N. Sh. El-Gendy, S. S. M. Mostafa, S. A. El-Temtamy, and A. I. Hashim, "Batch bioethanol production via the biological and chemical saccharification of some Egyptian marine macroalgae," *Journal of Applied Microbiology*, vol. 125, no. 2, pp. 422–440, 2018.

[13] R. Kooren, T. G. Sumithra, K. V. Jaseera et al., "A comparative study on pre-treatment methods for enhanced saccharification from tropical seaweeds to aid in bioethanol production," *Aquatic Botany*, vol. 184, Article ID 103594, 2023.

[14] J. J. Milledge and P. J. Harvey, "Golden tides: problem or golden opportunity? The valorization of *Sargassum* from beach inundations," *Journal of Marine Science and Engineering*, vol. 4, no. 3, p. 60, 2016.

[15] Z. R. Liang, F. J. Wang, X. T. Sun, W. J. Wang, and F. L. Liu, "Reproductive biology of *Sargassum thunbergii* (Fucales, Phaeophyceae)," *American Journal of Plant Sciences*, vol. 05, no. 17, pp. 2574–2581, 2014.

[16] H.-Y. Yeh, M.-C. Lee, M. J. H. Libatique, and Z.-H. Liao, "The effects of seawater temperature and irradiance on the sexual reproduction of *Sargassum ilicifolium* (Sargassaceae, Phaeophyta)," *Journal of Applied Phycology*, vol. 32, no. 1, pp. 661–670, 2020.

[17] Annual Book of American Society for Testing Materials (Astm) Standards, "Section 11, water and environmental technology," *01 Water (I) and 11.02 Water (II)*, vol. 11, 2009.

[18] APHA, *Standard Methods for the Examination of Water and Wastewater*, A. D. Eaton and M. A. H. Franson, Eds., American Public Health Association, Washington, DC, USA, 21st edition, 2005.

[19] AOAC, *Official Methods of Analysis*, K. Helrich and V. A. Arlington, Eds., Association of Official Analytical Chemists, Washington DC, USA, 17th edition, 2000.

[20] "ASTM D5865/D5865M-19. Standard test method for gross calorific value of coal and coke," 2011.

[21] "European Standard EN15402: solid recovered fuels—determination of the content of volatile matter," 2011.

[22] "European Standard EN15403/2011, Solid recovered fuels—determination of ash content," 2011.

[23] "European Standard EN15414-3/2011, Solid recovered fuels—determination of moisture content using the oven dry method—part 3: moisture in general analysis sample," 2011.

[24] A. H. Moubasher, S. I. I. Hafez, H. M. Aboelfattah, and A. M. Moharrarh, "Fungi of wheat and broad bean straw composts. II. Thermophilic fungi," *Mycopathologia*, vol. 78, no. 3, pp. 169–176, 1984.

[25] N. Sh. El-Gendy, H. N. Nassar, A. R. Ismail et al., "Fully integrated biorefinery process for the valorization of *Ulva fasciata* into different green and sustainable value-added products," *Sustainability*, vol. 15, no. 9, p. 7319, 2023.

[26] A. J. Walkley and I. A. Black, "Estimation of soil organic carbon by the chromic acid titration method," *Soil Science*, vol. 37, no. 1, pp. 29–38, 1934.

[27] M. L. Jackson, *Soil Chemical Analysis*, Prentice Hall of India Private Limited, New Delhi, India, 2nd edition, 1973.

[28] H. D. Chapman and P. F. Pratt, "Methods of analysis for soils, plants, and waters," *Division of Agriculture Sciences*, University of California, Berkeley, CA, USA, 1961.

[29] F. S. Watanabe and S. R. Olsen, "Test of an ascorbic acid method for determining phosphorus in water and $NaHCO_3$ extracts from soil," *Soil Science Society of America Journal*, vol. 29, no. 6, pp. 677-678, 1965.

[30] J. J. Benton Jr., *Laboratory Guide for Conducting Soil Test and Plant Analysis*, CRC Press, Boca Raton, FL, USA, 2001.

[31] B. Trica, C. Delattre, F. Gros et al., "Extraction and characterization of alginate from an edible brown seaweed (*Cystoseira barbata*) harvested in the Romanian Black Sea," *Marine Drugs*, vol. 17, no. 7, p. 405, 2019.

[32] N. Trivedi, R. S. Baghel, J. Bothwell et al., "An integrated process for the extraction of fuel and chemicals from marine macroalgal biomass," *Scientific Reports*, vol. 6, no. 1, Article ID 30728, 2016.

[33] G. A. Ismail, "Biochemical composition of some Egyptian seaweeds with potent nutritive and antioxidant properties," *Food Science and Technology*, vol. 37, no. 2, pp. 294–302, 2017.

[34] L. Ktari, C. Mdallel, B. Aoun, L. Chebil Ajjabi, and S. Sadok, "Fucoxanthin and phenolic contents of six dictyotales from the tunisian coasts with an emphasis for a green extraction using a supercritical CO_2 method," *Frontiers in Marine Science*, vol. 8, Article ID 647159, 2021.

[35] M. M. Ismail, G. M. El Zokm, and J. M. Miranda Lopez, "Nutritional, bioactive compounds content, and antioxidant activity of brown seaweeds from the Red Sea," *Frontiers in Nutrition*, vol. 10, Article ID 1210934, 2023.

[36] M. A. Abo-State, A. M. E. Ragab, N. Sh. El-Gendy, L. A. Farahat, and H. R. Madian, "Effect of different pretreatments on Egyptian sugar-cane bagasse saccharification and bioethanol production," *Egyptian Journal of Petroleum*, vol. 22, no. 1, pp. 161–167, 2013.

[37] A. Caro, K. Boltes, P. León, and E. García-Calvo, "Dibenzothiophene biodesulfurization in resting cell conditions by aerobic bacteria," *Biochemical Engineering Journal*, vol. 35, no. 2, pp. 191–197, 2007.

[38] L. J. Wickerhams, in *Taxonomy of Yeasts*, US Department of Agriculture, Washington, DC, USA, 1951.

[39] E. Y. Bridson, *Oxoid, Manual of Culture Media, Ingredients and Other Laboratory Services*, Oxoid Ltd, Basingstoke, UK, 9th edition, 2006, https://www.oxoid.com.

[40] A. H. Bahkali, "Production of cellulase, xylanase and polygalacturonase by *Verticillium tricorpus* on different substrates," *Bioresource Technology*, vol. 51, no. 2–3, pp. 171–174, 1995.

[41] G. L. Miller, "Use of dinitrosalicylic acid reagent for determination of reducing sugar," *Analytical Chemistry*, vol. 31, no. 3, pp. 426–428, 1959.

[42] R. Devereux and S. G. Willis, "Amplification of ribosomal RNA sequences," in *Molecular Microbial Ecology Manual*, A. D. L. Akkermans, J. D. Elsas, and F. J. Bruijn, Eds., pp. 277–287, Springer Science+Business Media Dordrecht, Berlin, Germany, 1995.

[43] T. J. White, T. Bruns, S. Lee, and J. Taylor, "Amplification and direct sequencing of fungal ribosomal rna genes for phylogenetics," in *PCR Protocols: A Guide to Methods and Applications*, M. A. Innis, D. H. Gelfand, J. J. Sninsky, and T. J. White, Eds., pp. 315–322, Academic Press, Inc, Cambridge, MA, USA, 1990.

[44] M. Gardes and T. D. Bruns, "ITS primers with enhanced specificity for basidiomycetes - application to the

6418, 2024, 1, Downloaded from https://onlinelibrary.wiley.com/doi/10.1155/2024/5184399 by Egyptian National Sci. Network (Enstinet), Wiley Online Library on [25/10/2024]. See the Terms and Conditions (https://onlinelibrary.wiley.com/terms-and-conditions) on Wiley Online Library for rules of use; OA articles are governed by the applicable Creative Commons License

identification of mycorrhizae and rusts," *Molecular Ecology*, vol. 2, pp. 113–118, 1993.

[45] M. A. Lodhi, G. N. Ye, N. F. Weeden, and B. I. Reisch, "A simple and efficient method for DNA extraction from grapevine cultivars and Vitis species," *Plant Molecular Biology Reporter*, vol. 12, no. 1, pp. 6–13, 1994.

[46] G. Zeng, H. You, K. Wang et al., "Semi-simultaneous saccharification and fermentation of ethanol production from *Sargassum horneri* and biosorbent production from fermentation residues," *Waste and Biomass Valorization*, vol. 11, no. 9, pp. 4743–4755, 2020.

[47] N. Jeyakumar, A. T. Hoang, S. Nižetić et al., "Experimental investigation on simultaneous production of bioethanol and biodiesel from macro-algae," *Fuel*, vol. 329, Article ID 125362, 2022.

[48] E. Aparicio, R. M. Rodríguez-Jasso, C. D. Pinales-Márquez et al., "High-pressure technology for *Sargassum* spp biomass pretreatment and fractionation in the third generation of bioethanol production," *Bioresource Technology*, vol. 329, Article ID 124935, 2021.

[49] A. Kumar, A. R. Chowdhuri, D. Laha, T. K. Mahto, P. Karmakar, and S. K. Sahu, "Green synthesis of carbon dots from *Ocimum sanctum* for effective fluorescent sensing of Pb^{2+} ions and live cell imaging," *Sensors and Actuators B: Chemical*, vol. 242, pp. 679–686, 2017.

[50] I. B. M. Ibraheem, R. M. Alharbi, N. Abdel-Raouf, and N. M. Al-Enazi, "Contributions to the study of the marine algae inhabiting Umluj seashore, Red Sea," *Beni-Suef University Journal of Basic and Applied Sciences*, vol. 3, no. 4, pp. 278–285, 2014.

[51] I. B. M. Ibraheem, S. H. Hamed, A. A. Abd elrhman, F. M. Farag, and N. Abdel-Raouf, "Antimicrobial activities of some brown macroalgae against some soil borne plant pathogens and in vivo management of *Solanum melongena* root diseases," *Australian Journal of Basic and Applied Sciences*, vol. 11, no. 5, pp. 157–168, 2017, https://www.ajbasweb.com/old/ajbas/2017/April/157-168.pdf.

[52] W. A. Fouda, W. M. Ibrahim, A. M. Ellamie, and G. Ramadan, "Biochemical and mineral compositions of six brown seaweeds collected from Red Sea at Hurghada Coast," *Indian Journal of Marine Sciences*, vol. 48, no. 4, pp. 484–549, 2019, https://core.ac.uk/download/pdf/297999427.pdf.

[53] E. Egaas and A. Varanis, "Effects of polychlorinated biphenyls and environmental temperature on in vitro formation of benzo[a]pyrene metabolites by liver of trout (Salmo gairdneri). Bio," *Chemical and Pharmaceutical Bulletin*, vol. 31, no. 4, pp. 561–566, 1982.

[54] A. S. Abdelmongy and K. M. El-Moselhy, "Seasonal variations of the physical and chemical properties of seawater at the Northern Red Sea, Egypt," *Open Journal of Ocean and Coastal Sciences*, vol. 2, no. 1, pp. 1–17, 2015.

[55] M. Z. Nassar, N. G. S. El-Din, and S. M. Gharib, "Phytoplankton variability in relation to some environmental factors in the eastern coast of Suez Gulf, Egypt," *Environmental Monitoring and Assessment*, vol. 187, no. 10, pp. 648–718, 2015.

[56] J. A. S. Olivier, J. R. L. Canepa, D. G. Zarate et al., "Bioenergetic valorization of *Sargassum fluitans* in the Mexican Caribbean: the determination of the calorific value and washing mechanism," *AIMS Energy*, vol. 10, no. 1, pp. 45–63, 2022.

[57] A. F. Al-Sadek, B. K. Gad, H. N. Nassar, and N. S. El-Gendy, "Recruitment of long short-term memory for envisaging the higher heating value of valorized lignocellulosic solid biofuel: a new approach," *Energy Sources, Part A: Recovery, Utilization, and Environmental Effects*, pp. 1–17, 2021.

[58] International Organization for Standardization, "ISO 17225-1. Solid biofuels—fuel specifications and classes," vol. 56, 2014, https://www.iso.org/standard/59456.html.

[59] M. G. Borines, R. L. de Leon, and J. L. Cuello, "Bioethanol production from the macroalgae *Sargassum* spp," *Bioresource Technology*, vol. 138, pp. 22–29, 2013.

[60] H. I. Mansour, H. R. Madian, L. A. Farahat, E. A. Hoballah, and M. K. Ibrahim, "Isolation of different clostridium isolates for acetone-butanol-ethanol (ABE) Production from Sargassum sp. Egypt," *Journal of Chemistry*, vol. 63, no. 1, pp. 4261–4272, 2020.

[61] S. Kavitha, T. Gajendran, K. Saranya, and V. Manivasagan, "Bioconversion of *Sargassum wightii* to ethanol via consolidated bioprocessing using *Lachnoclostridium phytofermentans* KSM 1203," *Fuel*, vol. 347, Article ID 128465, 2023.

[62] H. Kartikaningsih, S. Dayuti, A. Tumulyadi, and R. S. Umam, "Characteristics brown seaweed tea *Sargassum cristaefolium* from Talango Island, Madura, East Java," *AIP Conference Proceedings*, vol. 2120, Article ID 030016, 2019.

[63] A. Marín, M. Casas-Valdez, S. Carrillo et al., "The marine algae *Sargassum* spp. (Sargassaceae) as feed for sheep in tropical and subtropical regions," *Revista de Biologia Tropical*, vol. 57, no. 4, pp. 1271–1281, 2009.

[64] Y. L. Dewi, A. Yuniza, K. Sayuti, and M. E. Mahata, "Immersion of *Sargassum binderi* seaweed in river water flow to lower salt content before use as feed for laying hens," *International Journal of Poultry Science*, vol. 17, no. 1, pp. 22–27, 2018.

[65] A. Lopez-Santamarina, J. M. Miranda, A. d. C. Mondragon et al., "Potential use of marine seaweeds as prebiotics: a review," *Molecules*, vol. 25, no. 4, p. 1004, 2020.

[66] Y. L. Dewi, A. Yuniza, K. Sayuti, and M. E. Mahata, "Processing of *Sargassum binderi* seaweed for supplementation in poultry diet," *Journal of World's Poultry Research*, vol. 13, no. 1, pp. 103–111, 2023.

[67] S. R. Dalal, M. H. Hussein, N. E. El-Naggar, S. I. Mostafa, and S. A. Shaaban-Dessuuki, "Characterization of alginate extracted from *Sargassum latifolium* and its use in Chlorella vulgaris growth promotion and riboflavin drug delivery," *Scientific Reports*, vol. 11, no. 1, Article ID 16741, 2021.

[68] S. M. Mohy El-Din, "Utilization of seaweed extracts as biofertilizers to stimulate the growth of wheat seedlings," *The Egyptian Journal of Experimental Biology*, vol. 1, no. 1, pp. 31–39, 2015, https://www.ejmanager.com/mnstemps/15/15-1431728110.pdf.

[69] S. H. Mahmoud, D. M. Salama, A. M. M. El-Tanahy, and E. H. Abd El-Samad, "Utilization of seaweed (*Sargassum vulgare*) extract to enhance growth, yield and nutritional quality of red radish plants," *Annals of Agricultural Science*, vol. 64, no. 2, pp. 167–175, 2019.

[70] B. Bharath, K. Perinbam, S. Nirmalraj, and M. Mahendrakumar, "Biofertilizing efficiency *of Sargassum polycystum* extract on growth and biochemical composition of *Vigna radiata* and *Vigna mungo*," *Asian Pacific Journal of Reproduction*, vol. 7, no. 1, pp. 27–32, 2018.

[71] Y. Yao, X. Wang, B. Chen, M. Zhang, and J. Ma, "Seaweed extract improved yields, leaf photosynthesis, ripening time, and net returns of tomato (*Solanum lycopersicum* Mill.)," *ACS Omega*, vol. 5, no. 8, pp. 4242–4249, 2020.

[72] A. Adderley, S. Wallace, D. Stubbs et al., "*Sargassum* sp. as a biofertilizer: is it really a key towards sustainable

6418, 2024, 1, Downloaded from https://onlinelibrary.wiley.com/doi/10.1155/2024/5184399 by Egyptian National Sci. Network (Enstinet), Wiley Online Library on [25/10/2024]. See the Terms and Conditions (https://onlinelibrary.wiley.com/terms-and-conditions) on Wiley Online Library for rules of use; OA articles are governed by the applicable Creative Commons License

agriculture for the Bahamas?" *Bulletin of the National Research Centre*, vol. 47, no. 1, p. 112, 2023.

[73] B. T. K. A. Ilhami, S. Abidin, N. W. R. Martyasari et al., "Measurement of macroalgae total carbohydrate content found in Lendang Luar coast, Lombok, Indonesia for potential sources of bioethanol," *IOP Conference Series: Earth and Environmental Science*, vol. 913, Article ID 012077, 2021.

[74] R. Indrawati, H. Sukowijoyo, R. D. E. Wijayanti, and L. Limantara, "Encapsulation of brown seaweed pigment by freeze drying: characterization and its stability during storage," *Procedia Chemistry*, vol. 14, pp. 353–360, 2015.

[75] W. H. Yip, L. S. Joe, W. A. W. Mustapha, M. Y. Maskat, and M. Said, "Characterisation and stability of pigments extracted from *Sargassum binderi* obtained from Semporna," *Sabah. Sains Malaysiana*, vol. 43, no. 9, pp. 1345–1354, 2014.

[76] S. Rahmawati, R. Haryatfrehni, A. Meilianda, M. Nuhamunada, L. Pradani, and B. L. Prakasa, "Pigments characterization of macroalgae in Drini beach, Gunungkidul, Yogyakarta for systematics study," *KnE Life Sciences*, vol. 2, no. 1, pp. 294–299, 2015.

[77] M. Martins, L. M. d. S. Mesquita, B. M. C. Vaz et al., "Extraction and fractionation of pigments from Saccharina latissima (Linnaeus, 2006) using an ionic liquid + oil + water system," *ACS Sustainable Chemistry and Engineering*, vol. 9, no. 19, pp. 6599–6612, 2021.

[78] R. H. Haryatfrehni, S. C. Dewi, A. Meilianda, S. Rahmawati, and I. Z. R. Sari, "Preliminary study the potency of macroalgae in *Yogyakarta*: extraction and analysis of algal pigments from common *Gunung Kidul* seaweeds," *Procedia Chemistry*, vol. 14, pp. 373–380, 2015.

[79] G. Sanger, D. Wonggo, L. A. D. Y. Montolalu, and V. Dotulong, "Pigments constituents, phenolic content and antioxidant activity of brown seaweed *Sargassum* sp," *IOP Conference Series: Earth and Environmental Science*, vol. 103, Article ID 012057, 2022.

[80] Y. Sulistiyani, A. Sabdono, N. Afiati, and H. Haeruddin, "Fucoxanthin identification and purification of brown algae commonly found in Lombok Island, Indonesia," *Biodiversitas*, vol. 22, no. 3, pp. 1527–1534, 2021.

[81] N. A. S. Din, A. S. Mohd Alayudin, N.-S. Sofian-Seng et al., "Brown algae as functional food source of fucoxanthin: a review," *Foods*, vol. 11, no. 15, p. 2235, 2022.

[82] C. Lourenço-Lopes, M. Fraga-Corral, C. Jimenez-Lopez et al., "Biological action mechanisms of fucoxanthin extracted from algae for application in food and cosmetic industries," *Trends in Food Science and Technology*, vol. 117, pp. 163–181, 2021.

[83] B. Larsen, D. M. S. A. Salem, M. A. E. Sallam, M. M. Mishrikey, and A. I. Beltagy, "Characterization of the alginates from algae harvested at the Egyptian Red Sea coast," *Carbohydrate Research*, vol. 338, no. 22, pp. 2325–2336, 2003.

[84] C. S. D. Costa, S. L. Cardoso, E. Nishikawa, M. G. A. Vieira, and M. G. C. da Silva, "Characterization of the residue from double alginate extraction from *Sargassum filipendula* seaweed," *Chemical Engineering Transactions*, vol. 52, pp. 133–138, 2016.

[85] R. Kusumawati, J. Basmal, and B. S. B. Utomo, "Physicochemical characteristics of sodium alginate extracted from *Turbinaria* sp. and *Sargassum* sp," *Squalen Bulletin of Marine and Fisheries Postharvest and Biotechnology*, vol. 13, no. 2, pp. 79–84, 2018.

[86] D. A. Mohamed, A. A. Hassan, M. T. Ibrahim, and M. M. Helmy, "Extraction and characterization of sodium alginates extracted from *Sargassum muticum* and *Turbinaria conoides*," *International Journal of Innovative Science Engineering and Technology*, vol. 8, no. 1, pp. 2348–7968, 2021, https://ijiset.com/vol8/v8s1/IJISET_V8_I01_08.pdf.

[87] J. M.-L. Kok and C.-L. Wong, "Physicochemical properties of edible alginate film from Malaysian *Sargassum polycystum* C. Agardh," *Sustainable Chemistry and Pharmacy*, vol. 9, pp. 87–94, 2018.

[88] Y. Ardalan, M. Jazini, and K. Karimi, "*Sargassum angustifolium* brown macroalga as a high potential substrate for alginate and ethanol production with minimal nutrient requirement," *Algal Research*, vol. 36, pp. 29–36, 2018.

[89] N. Dharmayanti, J. Supriatna, A. Abinawanto, and Y. Yasman, "Isolation and partial characterization of alginate extracted from *Sargassum polycystum* collected from three habitats in Banten, Indonesia," *Biodiversitas*, vol. 20, no. 6, pp. 1776–1785, 2019.

[90] R. Benfares, M. Bouarab, A. Kord, S. Benrabah, and H. Seridi, "Characterization of alginates from four species of brown algae of the Algerian coast," no. 6, pp. 95–103, 2017.

[91] M. Aprilliza, "Characterization and properties of sodium alginate from brown algae used as an ecofriendly superabsorbent," *IOP Conference Series: Materials Science and Engineering*, vol. 188, Article ID 012019, 2017.

[92] N. Kavitha, T. P. Karunya, S. Kanchana et al., "Formulation of alginate based hydrogel from brown seaweed, *Turbinaria conoides* for biomedical applications," *Heliyon*, vol. 5, Article ID e02916, 2019.

[93] D. Fang, Y. Liu, S. Jiang, J. Nie, and G. Ma, "Effect of intermolecular interaction on electrospinning of sodium alginate," *Carbohydrate Polymers*, vol. 85, no. 1, pp. 276–279, 2011.

[94] S. Kaidi, Z. Belattmania, F. Bentiss, C. Jama, A. Reani, and B. Sabour, "Synthesis and characterization of silver nanoparticles using alginate from the brown seaweed *Laminaria ochroleuca*: structural features and antibacterial activity," *Biointerface Research in Applied Chemistry*, vol. 12, no. 5, pp. 6046–6057, 2022.

[95] P. Sundarrajan, P. Eswaran, A. Marimuthu, L. B. Subhadra, and P. Kannaiyan, "One pot synthesis and characterization of alginate stabilized semiconductor nanoparticles," *Bulletin of the Korean Chemical Society*, vol. 33, no. 10, pp. 3218–3224, 2012.

[96] D. J. Indrani and E. Budianto, "A study of extraction and characterization of alginates obtained from brown macroalgae *Sargassum duplicatum* and *Sargassum crassifolium* from Indonesia," *Dental Journal*, vol. 46, no. 2, pp. 65–70, 2013.

[97] M. A. Aguanza, R. Lauzon, and I. Emnace, "Extraction process optimization of sodium alginate from samu (*Sargassum piluleferum*) and evaluation of its stabilizing property for the production of sweetpotato (*Ipomoea batatas* L) beverage," *European Chemical Bulletin*, vol. 12, pp. 5128–5146, 2023.

[98] M. A. Fawzy, M. Gomaa, A. F. Hifney, and K. M. Abdel-Gawad, "Optimization of alginate alkaline extraction technology from *Sargassum latifolium* and its potential antioxidant and emulsifying properties," *Carbohydrate Polymers*, vol. 157, pp. 1903–1912, 2017.

[99] A. O. R. Nurhadini and Y. Setiawan, "Sodium alginate extraction from brown seaweed (*Turbinaria conoides*) and its structural property as bipolymer electrolyte," *Advances in Engineering Research*, vol. 167, pp. 170–172, 2019.

[100] N. Flórez-Fernández, H. Domínguez, and M. D. Torres, "A green approach for alginate extraction from *Sargassum muticum* brown seaweed using ultrasound-assisted

6418, 2024, 1, Downloaded from https://onlinelibrary.wiley.com/doi/10.1155/2024/5184399 by Egyptian National Sci. Network (Enstinet), Wiley Online Library on [25/10/2024]. See the Terms and Conditions (https://onlinelibrary.wiley.com/terms-and-conditions) on Wiley Online Library for rules of use; OA articles are governed by the applicable Creative Commons License

technique," *International Journal of Biological Macromolecules*, vol. 124, pp. 451–459, 2019.

[101] K. Sakugawa, A. Ikeda, A. Takemura, and H. Ono, "Simplified method for estimation of composition of alginates by FTIR," *Journal of Applied Polymer Science*, vol. 93, no. 3, pp. 1372–1377, 2004.

[102] M. A. Fawzy and M. Gomaa, "Optimization of citric acid treatment for the sequential extraction of fucoidan and alginate from *Sargassum latifolium* and their potential antioxidant and Fe(III) chelation properties," *Journal of Applied Phycology*, vol. 33, no. 4, pp. 2523–2535, 2021.

[103] S. Saji, A. Hebden, P. Goswami, and C. Du, "A brief review on the development of alginate extraction process and its sustainability," *Sustainability*, vol. 14, no. 9, p. 5181, 2022.

[104] K. I. Draget and C. Taylor, "Chemical, physical and biological properties of alginates and their biomedical implications," *Food Hydrocolloids*, vol. 25, no. 2, pp. 251–256, 2011.

[105] S. Jothisaraswathi, B. Babu, and R. Rengasamy, "Seasonal studies on alginate and its composition II: *Turbinaria conoides* (J.Ag.) Kütz. (fucales, phaeophyceae)," *Journal of Applied Phycology*, vol. 18, no. 2, pp. 161–166, 2006.

[106] R. V. Siriwardane, J. A. Poston, C. Robinson, and T. Simonyi, "Effect of additives on decomposition of sodium carbonate: precombustion CO_2 capture sorbent regeneration," *Energy and Fuels*, vol. 25, no. 3, pp. 1284–1293, 2011.

[107] R. Russo, M. Abbate, M. Malinconico, and G. Santagata, "Effect of polyglycerol and the crosslinking on the physical properties of a blend alginate-hydroxyethylcellulose," *Carbohydrate Polymers*, vol. 82, no. 4, pp. 1061–1067, 2010.

[108] A. Nesic, A. Onjia, S. Davidović et al., "Design of pectin-sodium alginate based films for potential healthcare application: study of chemico-physical interactions between the components of films and assessment of their antimicrobial activity," *Carbohydrate Polymers*, vol. 157, pp. 981–990, 2017.

[109] A. A. Bendaoudi, N. Boudouaia, S. Jellali et al., "Facile synthesis of double-cross-linked alginate-based hydrogel: characterization and use in a context of circular economy for cationic dye removal," *Waste Management & Research*, vol. 42, no. 6, pp. 495–507, 2023.

[110] S. Xu, A. Tabaković, X. Liu, D. Palin, and E. Schlangen, "Optimization of the calcium alginate capsules for self-healing asphalt," *Applied Sciences*, vol. 9, no. 3, p. 468, 2019.

[111] H. Doh and W. S. Whiteside, "Isolation of cellulose nanocrystals from brown seaweed, *Sargassum fluitans*, for development of alginate nanocomposite film," *Crystallization of Polymers*, vol. 3, no. 4, Article ID e10133, 2020.

[112] H. Doh, K. D. Dunno, and W. S. Whiteside, "Cellulose nanocrystal effects on the biodegradability with alginate and crude seaweed extract nanocomposite films," *Food Bioscience*, vol. 38, Article ID 100795, 2020.

[113] V. Cebrián-Lloret, M. Metz, A. Martínez-Abad et al., "Valorization of alginate-extracted seaweed biomass for the development of cellulose-based packaging films," *Algal Research*, vol. 61, Article ID 102576, 2022.

[114] Q. He, Q. Wang, H. Zhou et al., "Highly crystalline cellulose from brown seaweed *Saccharina japonica*: isolation, characterization and microcrystallization," *Cellulose*, vol. 25, no. 10, pp. 5523–5533, 2018.

[115] H. Amir and B. Siti Ari, "Effect of isolation method on characterization of microcrystalline cellulose from brown seaweed *Sargassum vulgare*," *Indonesian Journal of Pharmacy*, vol. 33, no. 1, pp. 42–51, 2022.

[116] J. Muthukumar and R. Chidambaram, "Isolation and quantification of cellulose from various food-grade macroalgal species," *Cellulose Chemistry and Technology*, vol. 57, no. 3-4, pp. 237–244, 2023.

[117] F. Jelani, G. Walker, and J. Akunna, "Effects of thermochemical and enzymatic pre-treatment of tropical seaweeds and freshwater macrophytes on biogas and bioethanol production," *International journal of Environmental Science and Technology*, vol. 20, no. 12, pp. 12999–13008, 2023.

[118] M. Yanagisawa, S. Kawai, and K. Murata, "Strategies for the production of high concentrations of bioethanol from seaweeds," *Bioengineered*, vol. 4, no. 4, pp. 224–235, 2013.

[119] S.-M. Lee and J.-H. Lee, "The isolation and characterization of simultaneous saccharification and fermentation microorganisms for *Laminaria japonica* utilization," *Bioresource Technology*, vol. 102, no. 10, pp. 5962–5967, 2011.

[120] A. S. Zaky, D. Greetham, E. J. Louis, G. A. Tucker, and C. Du, "A new isolation and evaluation method for marine-derived yeast spp. with potential applications in industrial biotechnology," *Journal of Microbiology and Biotechnology*, vol. 26, no. 11, pp. 1891–1907, 2016.

[121] M. Mulet, M. Gomila, J. Lalucat, R. Bosch, R. Rossello-Mora, and E. García-Valdés, "*Stutzerimonas* decontaminans sp. nov. isolated from marine polluted sediments," *Systematic and Applied Microbiology*, vol. 46, Article ID 126400, 2023.

[122] M. Kawaroe and I. Rusmana, "Production of bioethanol from macroalgae *Gelidium* sp. using agarase enzymes of marine bacteria," *International Journal of Environment and Bioenergy*, vol. 9, no. 3, pp. 243–251, 2014.

[123] K. K. Kadimpati, S. Thadikamala, K. Devarapalli, L. Banoth, and K. B. Uppuluri, "Characterization and hydrolysis optimization of *Sargassum cinereum* for the fermentative production of 3G bioethanol," *Biomass Conversion and Biorefinery*, vol. 13, no. 3, pp. 1831–1841, 2023.

[124] J. Chen, J. Bai, H. Li, S. Fang, and S. Fang, "Prospects for bioethanol production from macroalgae," *Trends in Renewable Energy*, vol. 1, no. 3, pp. 185–197, 2015.

[125] M. E. Elshobary, R. A. El-Shenody, and A. Abomohra, "Sequential biofuel production from seaweeds enhances the energy recovery: a case study for biodiesel and bioethanol production," *International Journal of Energy Research*, vol. 45, no. 4, pp. 6457–6467, 2020.

[126] A. Mewada, S. Pandey, S. Shinde et al., "Green synthesis of biocompatible carbon dots using aqueous extract of *Trapa bispinosa* peel," *Materials Science and Engineering: C*, vol. 33, no. 5, pp. 2914–2917, 2013.

[127] M. Wang, Y. Wan, K. Zhang et al., "Green synthesis of carbon dots using the flowers of *Osmanthus fragrans* (Thunb.) Lour. as precursors: application in Fe^{3+} and ascorbic acid determination and cell imaging," *Analytical and Bioanalytical Chemistry*, vol. 411, no. 12, pp. 2715–2727, 2019.

[128] D. Bhattacharya, M. K. Mishra, and G. De, "Carbon dots from a single source exhibiting tunable luminescent colors through the modification of surface functional groups in ORMOSIL films," *Journal of Physical Chemistry C*, vol. 121, no. 50, pp. 28106–28116, 2017.

[129] A. Dager, T. Uchida, T. Maekawa, and M. Tachibana, "Synthesis and characterization of mono-disperse carbon

6418, 2024, 1, Downloaded from https://onlinelibrary.wiley.com/doi/10.1155/2024/5184399 by Egyptian National Sci. Network (Enstinet), Wiley Online Library on [25/10/2024]. See the Terms and Conditions (https://onlinelibrary.wiley.com/terms-and-conditions) on Wiley Online Library for rules of use; OA articles are governed by the applicable Creative Commons License

quantum dots from fennel seeds: photoluminescence analysis using machine learning," *Scientific Reports*, vol. 9, Article ID 14004, 2019.

[130] M. Zaib, A. Akhtar, F. Maqsood, and T. Shahzadi, "Green synthesis of carbon dots and their application as photocatalyst in dye degradation studies," *Arabian Journal for Science and Engineering*, vol. 46, no. 1, pp. 437–446, 2021.

[131] B. T. Hoan, P. D. Tam, and V.-H. Pham, "Green synthesis of highly luminescent carbon quantum dots from lemon juice," *Journal of Nanotechnology*, vol. 2019, Article ID 2852816, 9 pages, 2019.

[132] H. Eskalen, M. Çeşme, S. Kerli, and S. Özğan, "Green synthesis of water-soluble fluorescent carbon dots from rosemary leaves: applications in food storage capacity, fingerprint detection, and antibacterial activity," *Journal of Chemical Research*, vol. 45, no. 5-6, pp. 428–435, 2021.

[133] S. Wu, W. Li, W. Zhou et al., "Large-scale one-step synthesis of carbon dots from yeast extract powder and construction of carbon dots/PVA fluorescent shape memory material," *Advanced Optical Materials*, vol. 6, no. 7, Article ID 1701150, 2018.

[134] Z. Lai, X. Guo, Z. Cheng, G. Ruan, and F. Du, "Green synthesis of fluorescent carbon dots from cherry tomatoes for highly effective detection of trifluralin herbicide in soil samples," *ChemistrySelect*, vol. 5, no. 6, pp. 1956–1960, 2020.

[135] W. A. Qureshi, B. Vivekanandan, J. A. Jayaprasath, D. Ali, S. Alarifi, and K. Deshmukh, "Antimicrobial activity and characterization of pomegranate peel-based carbon dots," *Journal of Nanomaterials*, vol. 2021, Article ID 9096838, 6 pages, 2021.

[136] X. Dong, W. Liang, M. J. Meziani, Y. P. Sun, and L. Yang, "Carbon dots as potent antimicrobial agents," *Theranostics*, vol. 10, no. 2, pp. 671–686, 2020.

[137] M. M. Al Awak, P. Wang, S. Wang, Y. Tang, Y. P. Sun, and L. Yang, "Correlation of carbon dots' light-activated antimicrobial activities and fluorescence quantum yield," *RSC Advances*, vol. 7, no. 48, pp. 30177–30184, 2017.

[138] M. Ghirardello, J. Ramos-Soriano, and M. C. Galan, "Carbon dots as an emergent class of antimicrobial agents," *Nanomaterials*, vol. 11, no. 8, p. 1877, 2021.

6418, 2024, 1, Downloaded from https://onlinelibrary.wiley.com/doi/10.1155/2024/5184399 by Egyptian National Sci. Network (Enstinet), Wiley Online Library on [25/10/2024]. See the Terms and Conditions (https://onlinelibrary.wiley.com/terms-and-conditions) on Wiley Online Library for rules of use; OA articles are governed by the applicable Creative Commons License